

Access and Management of Sweat for Non-Invasive Biomarker Monitoring: A Comprehensive Review

Tamoghna Saha ^{a,\$}, Rafael Del Caño ^{a,b,\$}, Ernesto De la Paz ^a, Samar S. Sandhu ^a, and Joseph Wang ^{a,*}

^aDepartment of Nanoengineering, University of California San Diego La Jolla, CA 92093, USA

^bDepartment of Physical Chemistry and Applied Thermodynamics, University of Cordoba, E-14014, Spain.

^{\$}Equal Contribution

*Corresponding author: josephwang@ucsd.edu

Keywords: Sweat, Biochemical Sensors, Wearable, Biomarkers, Health Monitoring

Abstract

Sweat is an important biofluid present in the body since it regulates the internal body temperature, is relatively easy to access on the skin unlike other biofluids and contains several biomarkers which are also present in the blood. Although sweat sensing devices have recently displayed tremendous progress, most of the emerging devices primarily focus on the sensor development, integration with electronics, wearability, and data from *in-vitro* studies and short-term on-body trials during exercise. To further the advances in sweat sensing technology, this review aims to present a comprehensive report on the approaches to access and manage sweat from the skin towards improved sweat collection and sensing. We begin by delineating the sweat secretion mechanism through the skin, and the historical perspective of sweat, followed by a detailed discussion on the mechanisms governing sweat generation and management on the skin. We conclude by presenting the advanced applications of sweat sensing, supported by a discussion of robust, extended-operation epidermal wearable devices aiming to strengthen personalized healthcare monitoring systems.

1. Introduction

This review will provide a comprehensive overview regarding the existing techniques used for withdrawing, sampling, and managing sweat from the skin surface. Unlike other biofluids (such as interstitial fluid (ISF), saliva, urine, and tears), human sweat remains relatively easy to access due to the following reasons: (a) sweat glands are distributed throughout the entire surface of the body (~ 2-4 million in total)^[1], which means that sweat can be generated from all body parts; and (b) sweat appears naturally on the skin surface to regulate the internal body temperature, which can get elevated through common activities such as exercise.^[2] Furthermore, since sweat contains important biomarkers which are also present in blood^[1,3], it appears to be an attractive non-invasive alternative biofluid source for gaining important health information regarding the human body. The on-demand availability of sweat on the skin surface has led to the development of several skin-worn non-invasive epidermal devices that allow continuous and convenient access to the health and nutritional state of the human body.^[4-9] The success and reliability of such sweat-based sensing and energy devices require a deep understanding of the sweat sampling methods and the factors that affect their efficiency for long-term monitoring.

Over the years, researchers have continuously investigated different active and passive non-invasive techniques for extracting sweat on the skin surface and how to deploy them through wearable prototypes. Active sweating through physical exertion has been the most common way till date to generate sweat instantaneously on the skin surface.^[1] Other techniques include thermal^[10] or chemical stimulation^[11], osmosis^[12,13], or relying on the natural perspiration rate of the human subject.^[14] Classical approaches for sweat sampling and transport include utilization of substrates such as absorbent pads^[15,16], and commercial Wescor Macroduct[®] patches.^[17] Additionally, the prototypes comprising surfaces with alternative superhydrophilic and superhydrophobic coatings^[18], and in-house fabricated microfluidic channels which are either polydimethylsiloxane (PDMS)^[8,19], paper^[13], or thread based, have been also utilized for the same purpose.^[20] Furthermore, efficient sweat management approaches for facilitating prolonged sweat collection and sensing have been achieved via inclusion of capillary valves for flow regulation^[7,21], evaporation^[22-24], or by increasing the surface area of the sampling zone in the prototypes.^[23] Sensing of various sweat biomarkers has been largely conducted with either electrochemical or colorimetric based assays.^[25] Moreover, sweat collection techniques have also benefited energy

harvesting applications, such as with skin-worn biofuel cells (BFCs).^[26,27] Hence, the sweat collection method should be tailored to meet requirements of the specific sensing or energy applications.

Herein, we discuss and summarize the different approaches used to date for continuous, long-term sweat withdrawal, sampling, and management, and discuss how these capabilities are executed in wearable sensing and energy platforms. To get a better understanding, we begin by discussing the physiological mechanism of sweat production inside the human body and the historical importance of sweat sensing. Subsequently, we provide a detailed analysis of existing sweat withdrawing techniques. Next, we focus on the different sweat management approaches that facilitate long-term sampling and epidermal sensing. Finally, we discuss future directions and prospects, with a focus towards state-of-the-art wearable epidermal devices and advanced sweat sensing applications. Overall, this review differentiates from existing sweat-based wearable sensor reviews by focusing primarily on key techniques and strategies for accessing and sampling the sweat biofluid towards the successful effective operation of such skin-worn sensors for supporting continuous and long-term monitoring.

1.1 Generation Mechanism and Historical Perspective of Sweat

To understand the different sweat withdrawal techniques, it is important to initially know regarding how sweat is generated on the skin surface. The human skin consists of three types of sweat glands: eccrine, apocrine, and apoeccrine (**Figure 1a left**).^[1,2] The eccrine sweat glands are located at the hypodermis section of the skin and are majorly responsible for sweat production in the body. The density of these glands are the highest ($\sim 250\text{-}550$ glands/cm²) and their total number ranges $\sim 2\text{-}4$ million in the entire body. Eccrine sweat glands consist of three sections: secretory coil, dermal duct, and upper coil duct. The secretory coil consists of three types of cell: clear, dark, and myoepithelial, in which the clear cells are majorly responsible for sweat production (**Figure 1a right**).^[2] Additionally, the dark cells act as a storage for the active materials in sweat, while the myoepithelial cells provide structural integrity to the duct against the hydrostatic pressure exerted by sweat. As the body experiences a thermal stimulation, an osmotic gradient gets generated in the clear cells due to influx of calcium ions (Ca²⁺), which causes water movement into the lumen section of the secretory coil (**Figure 1a panel 1**). Ions and salts are continuously absorbed and reabsorbed between the clear cells and lumen via active and passive diffusion processes. Hence,

the eccrine sweat is mainly composed of water, NaCl, and substances from the interstitial fluid (ISF). The rate of reabsorption varies inversely to the flow speed of sweat in the duct, indicating that the lower the absorption rate, the higher will be the electrolyte levels in the luminal sweat. The sweat from the luminal cells is then pumped along the duct (**Figure 1a panel 2**) via capillary forces towards the skin, where it appears on the skin surface through the skin pores.

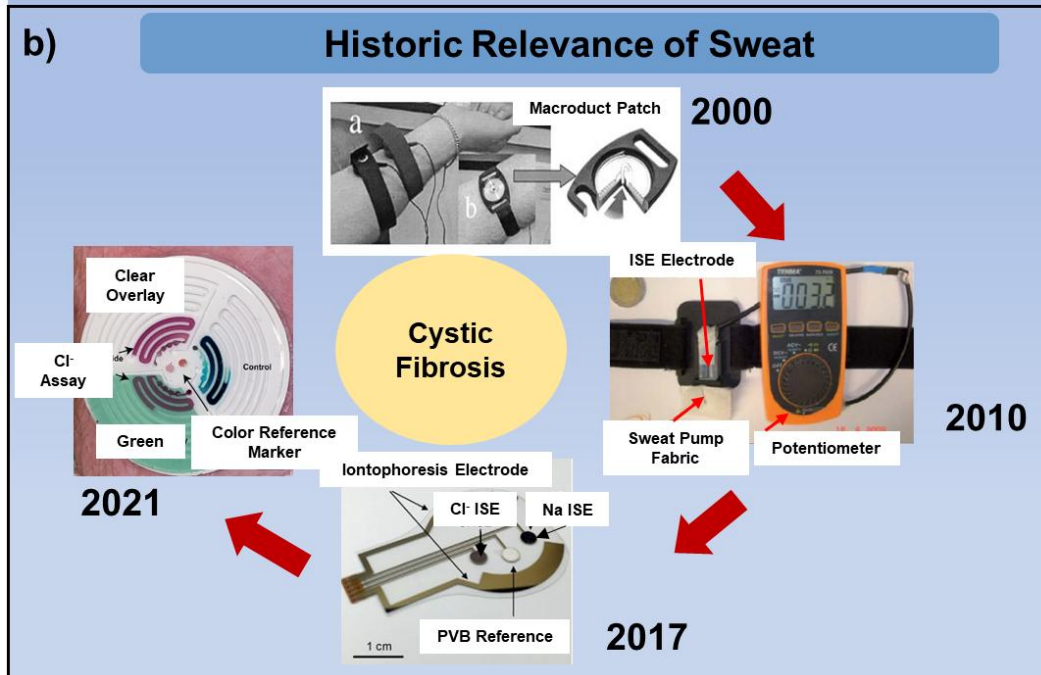
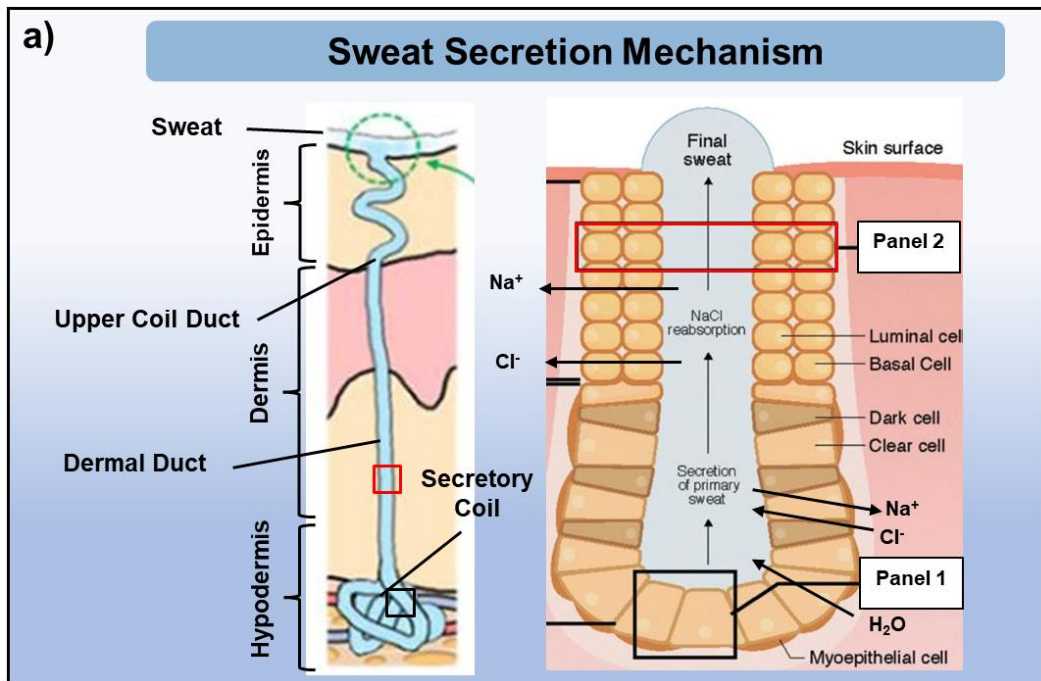


Figure 1. Sweat secretion mechanism and historical relevance of sweat sensing. a) Schematic showing the cross-section of the skin with the different types of sweat glands, and the mechanism of sweat secretion in the secretory coil.^[2,28] Adapted with permission. Copyright 2020, American Chemical Society and Copyright 2019, Taylor and Francis Group. b) Chronological evolution of sweat-based cystic fibrosis detecting prototypes.^[17,29–31] Adapted with permission. Copyright 2000, Wiley-VCH Verlag GmbH & Co. KGaA, Weinheim. Copyright 2010, Royal Society of Chemistry. Copyright 2017, National Academy of Sciences. Copyright 2021, American Association for the Advancement of Science.

The importance of measuring sweat biomarkers for health monitoring and disease detection has been a topic of interest for a very long time. Cystic fibrosis (CF) is one of the first health disorders to be investigated that contributes to irregular sweat electrolyte levels (usually Cl^- and Na^+).^[17,29,32] The Na^+ and Cl^- levels during CF can reach up to $\sim 60 \text{ mM}$ ^[29] and $\sim 160 \text{ mM}$ ^[31], respectively, with exercise. Under sedentary conditions, both Na^+ and Cl^- can range $\sim 80\text{-}100 \text{ mM}$ during CF, as compared to $20\text{-}30 \text{ mM}$ in healthy subjects.^[30] CF is an autosomal genetic disease that occurs due to mutations in the cystic fibrosis transmembrane conductance regulator (CFTR) gene.^[17] Due to the continuous and dynamic mutation of the CFTR gene, routine screening of CF has always proven to be challenging.^[33] Traditional techniques for CF detection include polymerase chain reaction (PCR), fluorometric based assays^[34], flame photometry, and anion exchange chromatography.^[17] However, since such techniques demand sophisticated, bulky, expensive analytical instrumentation with high degree of technical operational expertise with not being able to provide real-time analysis of biomarker levels, finding alternative wearable platforms for CF detection has received tremendous attention.

Iontophoresis (IP) using transdermal pilocarpine delivery has served as a gold standard sweat extraction method for decades since it is convenient, non-invasive, and patient friendly.^[35] Researchers started using this technique for CF detection by combining it with a Wescor Macroduct[®] patch for sweat sampling around early 2000's (**Figure 1b top**).^[17] The Macroduct patch consists of a blue dye in the tubing that provides an estimate of the sweat rate and volume sampled. The sampled sweat ($\sim 50\text{-}75 \mu\text{L}$) was routed through an ion-selective commercial microelectrode array for *ex-vivo* electrolyte estimation. Around 2010's, researchers started developing a wearable prototype version for CF detection (**Figure 1b right**). One such reported prototype included commercial fabrics for sampling exercise induced sweat and transporting it to the ion-selective electrodes (ISEs) for electrolyte sensing.^[29] A portable potentiometer was used to obtain a reading on a real-time scale. All these individual components were typically assembled

using a strap and worn on the body. The prototype showed Na^+ concentration around ~ 60 mM from CF patients with exercise. However, the presence of bulky components in such prototypes and the requirement of physical exertion prior the monitoring, led to the development of a fully integrated wearable platform in 2017 (**Figure 1b bottom**).^[30] Such epidermal platform included an iontophoretic platform for sweat extraction and Na^+ and Cl^- ISEs for specific electrolyte estimation. The whole system was even connected to a wireless circuit board, that allowed real-time estimation of electrolyte levels and sweat rate. IP could generate sweat rate up to ~ 1 $\mu\text{L}/\text{min}/\text{cm}^2$ and show sweat Na^+ and Cl^- concentration around ~ 80 - 100 mM in CF patients. On a similar note, a colorimetric based, soft epidermal microfluidic device for sweat Cl^- estimation was also developed last year for early CF diagnosis in a population of wide age range (**Figure 1b left**).^[31] The estimated Cl^- concentration ranged 80 - 160 mM in CF patients after exercise. Hence, it is evident that CF-based sweat sensors have evolved immensely over the last two decades, clearly highlighting the historical relevance of sweat and its potential to be used as an alternative biofluid source for non-invasive health monitoring and disease detection.

To get further in-depth information regarding the potential of sweat, the following sections of this review will summarize the different approaches used to date for continuous, long-term sweat withdrawal, sampling, and management, and discuss how these factors get executed in wearable sensing and energy platforms for advanced high-tech applications.

2. Sweat Generation Techniques on Skin

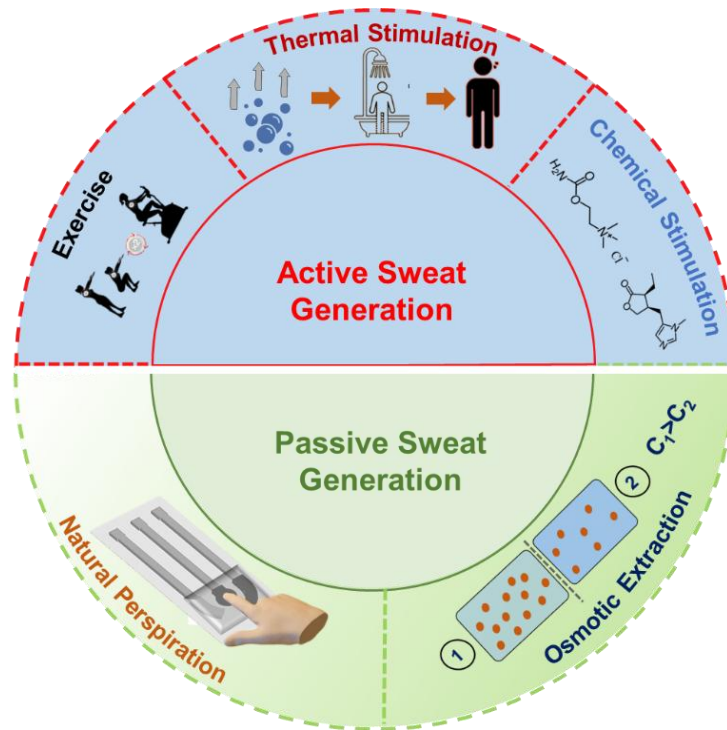


Figure 2: Schematic showing a compiled representation of different active and passive sweat withdrawal techniques reported to date.

To quantify the different biomarkers in sweat, the primary necessity is to first have the sweat fluid be accessible on the skin surface (**Figure 2**). The techniques through which sweat gets generated on the skin, can be broadly classified into two main categories: active and passive. Active sweat generation techniques are generally exhaustive for the human body as they rely on either physical exertion through exercise^[30,36–38], external heat application (through sauna or hot shower) on skin^[10,39], or on transdermal delivery of chlorogenic agents for triggering sweat production.^[40,41] Although these techniques usually end up generating higher sweat volume, the generated sweat remains susceptible to questions about clean capture, external contamination, losses due to uncontrolled evaporation, and dilution due to excessive sweating. On the contrary, passive sweat generation techniques are comforting to the body since their working principles do not involve applying an external stimulus. Relying on the natural sweat generation rate^[9,28,42–45] or by using an external medium for generating an osmotic pressure difference^[13,23,46–48] with respect to the sweat, have proven to be attractive for passive sweat extraction. While these techniques are exertion free, non-invasive, and can operate under low sweating conditions (such as at rest or low humidity settings), they sample low sweat volume over time which can be susceptible to losses

due to evaporation. Thus, all sweat withdrawing techniques possess their own advantages and disadvantages. The next section will provide a detailed discussion and analysis about the working mechanism of all sweat withdrawing techniques and will illustrate how they are executed in different wearable form factors for on-body sensing.

2.1 Sweat Generation via Active Sweating

A common way to generate instantaneous sweat on the skin surface is via active perspiration, where an applied external stimulus (heat, shock, or chemical) triggers the sweat production in the sweat glands. The working principles and the protocols used for this goal are shown in **Figure 3**. Active sweat generation through exercising (at varying intensity levels) is the conventional approach that researchers have predominantly used for on-body validation of various wearable prototypes, that aim to target the non-invasive detection of various biomarkers.^[4,8,19,33,38,49] The sensing component of such prototypes can be deployed in three different ways for facilitating continuous monitoring under active sweating: (a) direct interfacing with the sweat present on the skin surface^[4], (b) embedding inside microfluidic channels^[8], and (c) interfacing with external microfluidic form factors (polymer, paper, or thread based microfluidic channels).^[6] The example shown in **Figure 3a left** comprises of a soft, thin, flexible epidermal wearable tattoo with screen printed electrodes for sweat lactate estimation. Lactate is a byproduct of anaerobic glycolysis, commonly generated in sweat as an outcome of oxidative stress experienced by the body due to high levels of physical exertion.^[23] The NE-shaped tattoo comprises of the screen-printed three-electrode system with enzymatically (lactate oxidase, LOx) functionalized working electrodes for selective lactate detection.^[50] The patch was tested during active exercise for 2000 seconds where the sweat lactate concentration peaked up to ~ 20 mM. Although, direct interfacing allows the highest proximity of the sensor with skin, it can still make the sensor vulnerable to contamination from skin or be exposed to lesser biofluid volume due to losses from sweat evaporation, if not properly sealed.

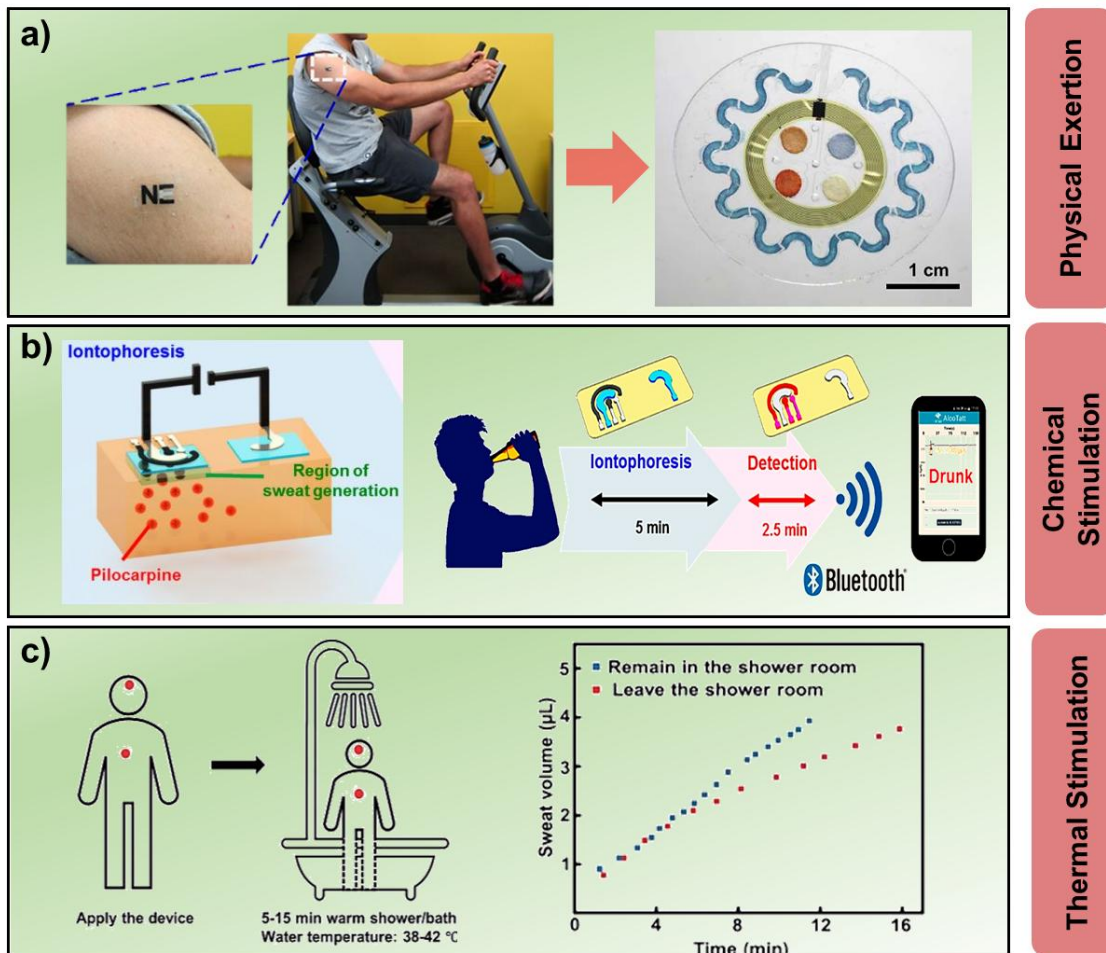


Figure 3: Active sweat withdrawal techniques. Sweat can be generated on the skin surface (a) through exhaustive physical exertion.^[8,50] Reproduced with permission. Copyright 2013, American Chemical Society and Copyright 2016, American Association for the Advancement of Science. (b) Use of iontophoresis for delivering chlorogenic agents for chemical stimulation,^[11] Reproduced with permission. Copyright 2016, American Chemical Society. Use of (c) using thermal stimulation techniques.^[40] Reproduced with permission. Copyright 2019, Royal Society of Chemistry.

Epidermal prototypes can also harvest and transport actively perspired sweat using conventional microfluidic channels (as implied by the arrow), with pre-immobilized reagents for specific sweat biomarker detection (**Figure 3a right**).^[21,39,51] Such prototypes are usually colorimetric based where an inflowing sweat biomarker undergoes a redox reaction to generate a colored product, whose intensity directly correlates with the amount of biomarker present, and can be quantified using smartphone-based imaging techniques. Unlike the disadvantages (limited only to lab settings, time consuming to apply, blocking of sweat glands) of common of sweat sampling

methods (whole body washdown, patches, and polymer bags)^[52], microfluidic channels allow better fluid control under limited operating space. The prototype shown in **Figure 3a right** was based on such similar principles, where it could simultaneously measure glucose, chloride, lactate, pH, and sweat rate from subjects during active exercise (cycling and outdoor activities).^[8] Several other reported wearable prototypes also function based on similar principles.^[7,21,39,51,53–55] Finally, the sensing zone can be also interfaced directly to the microfluidic pathway. In such a case, the incoming biomarker from the actively generated sweat undergoes a continuous reaction to generate real-time trends of the biomarker levels.^[5,6,41,56–59] Although, microfluidic channels allow rapid sampling, operation with low reagent volume, better control of molecules due to laminar flow, and the feasibility of including automation to avoid human error^[60,61], they can still be exposed to biofouling from sweat. Moreover, under high sweat rate, the immobilized reagents for the colorimetric assays within the microfluidic channels can also be susceptible to leaching, which might consequently dampen the biomarker signal. Multiple common sweat biomarkers, such as glucose, lactate, sodium, chloride, uric acid, or ascorbic acid, have been measured using this arrangement. However, since exercise involves physical exertion, it might not be the best testing methodology for deriving information from sweat from subjects who are aged and suffer from pre-existing health conditions. Hence, other alternative sweat withdrawing techniques that would demand lesser exertion and be comforting to the human body are highly desired.

Given the limitations of sweat withdrawal via exercise, researchers have used chemical^[40,41] and thermal stimulation techniques^[10,39] as other non-invasive alternatives for sweat extraction. Cholinergic agents, such as pilocarpine or carbachol, have proven to induce sweat secretion in the secretory coils of the sweat glands (chemical stimulation).^[62] These agents are cationic compounds which are transdermally delivered through the skin surface via IP. IP is an established technique for inducing fluid flow inside the skin using electric field (**Figure 3b**). During IP, these agents are loaded (usually in a hydrogel) onto the anodic terminal and delivered through the skin by applying an external electric current (0.2-0.5 mA/cm²), which consequently triggers the movement of the anionic species inside the skin towards the anode and cationic/neutral species towards the cathode (direction of electroosmotic flow). The sensing component can be placed on either of the electrode terminal, depending upon the electrostatic nature of the target biomarker. Moreover, the volume of sweat generated can range 15-100 μ L, depending on the applied current density and IP time.^[63] The schematic shown in **Figure 3b** describes a soft,

adhesive tattoo like wearable patch for sweat alcohol sensing using IP.^[11] The patch consisted of two silver electrodes for applying IP and an enzymatic (alcohol oxidase (AOx)) electrochemical sensor (with a catalytic Prussian blue (PB) layer) attached near one of the electrode terminal, which could measure alcohol levels up to 40 mM *in-vitro*. The patch was validated on subjects after letting them consume varying levels (5-10 oz) of alcohol beverages. With 5 mins of IP, the sensor was able to give the response for alcohol presence in sweat and show a good correlation with blood alcohol concentration (BAC). Similar patches working with IP have also been developed for other biomarkers such as electrolytes^[30,64], vitamin C^[9], glucose^[41,65], amino acids^[66] and lactate.^[67] Although IP can operate on subjects at rest, there always remains a possibility of skin burns due to electric current and drug overdosing due to material defects in the patch, hence requiring proper safety precautions.^[68] The power requirement to generate electricity also remains as a major concern.

The thermal stimulation technique for sweat generation is accomplished by exposing the body to high temperature conditions (such as hot shower or sauna bath).^[7,10,39] Such an external stimulus raises the internal body temperature which eventually leads to greater sweat generation for homeostasis maintenance. The schematic shown in **Figure 3C** shows the testing protocol followed by a prototype during on-body testing, that relies on warm shower for sweat generation. The prototype following this protocol relied on colorimetric measurements of measuring pH, urea, and creatinine concentrations along with the sweat rate.^[10] 5-15 mins of hot shower were sufficient for sensing sweat biomarkers. The plot in **Figure 3C** also verifies that higher the exposed temperature, the higher will be the rate of sweat generation. Such similar approaches have been also used by other colorimetric platforms for measuring nutritional biomarkers (calcium, zinc, and vitamin C, with 50 mins sauna)^[39], lactate, and electrolytes (with 30-40 mins sauna) in sweat.^[7] Since, thermal stimulation techniques generate high sweat rates ($\sim 0.3-0.5 \mu\text{L}/\text{min}$), they are mostly used in conjunction with microfluidic platforms, as they allow better sweat fluid management. Although this technique does not include exhaustive physical exertion, long-term exposure of the skin to such high temperatures could prove detrimental to the skin.^[69] Moreover, the concerns similar to active sweating and leaching in microfluidic channels also remain valid in this case. Hence, the next section will focus on passive sweat extraction techniques which are comforting to the body.

2.1 Sweat Generation via Passive Sweating

As an alternative to the cumbersome and stressful active perspiration techniques, researchers have come up with sweat generation techniques which are exertion free and comforting to the body. In one such technique, the concept of diffusion has been utilized to sample sweat biomarkers. The working principle used for this passive sweating technique is shown in **Figure 4**. This concept was pioneered in 2019, where the fingertip was used for *ex-situ* sweat lactate measurements using an agarose based hydrogel on rested subjects.^[14] The hydrogel acted as a sweat reservoir that facilitated lactate transport (due to its inherent water content) from the fingertip to the sensing electrodes, based on the natural perspiration rate. Moreover, the fingertip was chosen as the sampling site since it was found to be extremely rich with sweat glands and have close proximity to the blood capillaries.^[70,71] Potentiometry with carbon electrodes was used in this study. This concept was later translated into a fully integrated prototype for *ex-situ* caffeine and lactate measurements from the fingertip of rested subjects.^[28] The reported prototype used Au electrodes with multi-walled carbon nanotubes (MWCNTs) and poly-m-phenylenediamine (PPD) for sensing, connected to a physical circuit board (PCB) on bench, that allowed direct data storage on cloud. Although estimating caffeine and lactate levels from sweat at rest are important, nothing can beat the fact of this concept being transitioned for sweat glucose estimation without any active perspiration requirement.

The first touch-based prototype for sweat glucose measurement was developed in 2021 (**Figure 4a**).^[43] Unlike the previous reported touch based prototypes^[14,28], this prototype used a porous polyvinyl alcohol (PVA) hydrogel (75 μm thickness) for sampling and transporting glucose from the fingertip to the sensor (PB based carbon ink). PVA based hydrogels are more porous than agarose gels.^[72,73] Hence, such a gel type allowed faster (within 60 sec) biomarker transport which could be useful for glucose sensing, since its amount in sweat is low (unlike blood). The prototype was able to show an increase in the sweat glucose level after meal intake, along with validations from blood glucose. Since the correlation between sweat and blood glucose has always remained debatable, the researchers developed an algorithm to eliminate the dependency on interpersonal sweat rate for their concentration calculations. Such personal calibration led to greatly enhanced the correlation (Pearson's correlation coefficient (Pr)=0.95, with mean absolute relative difference (MARD)~ 7.9%, and 100% points lying in the A+B region of Clarkes Error Grid (CEG)) between

the estimated sweat and blood glucose concentration. The same group has expanded these principles towards levodopa (L-dopa) monitoring in sweat^[44], and cortisol^[42] in connection to enzymatic (tyrosinase) and molecularly-imprinted (MIP) receptors, respectively, – a major milestone for sweat sensing. The former allowed tracking of L-Dopa pharmacokinetic profiles following an oral tablet administration. The passive fingertip perspiration was also applied to biofuel cell energy harvesting using sweat lactate as the fuel.^[26] Remarkably high ‘return of investment’ was reported considering the passive nature of the sweat generation. Although finger touch-based sensing provides rapid, painless, non-invasive monitoring from sweat, it still suffers from a few potential drawbacks such as: (a) Since there is a hydrogel involved which is kept open (without concealment) during sensing, it can be vulnerable to drying over time. Drying would reduce the water content of the hydrogel that would eventually disrupt the biomarker transport, induce noise in the system, and not support long-term monitoring; (b) No prototype has been able to quantify the sweat rate/sweat volume while sensing. These are useful parameters whose estimation could give an idea about the extent of dilution caused by the water in the hydrogel; (c) The hydrogel thickness is crucial since it controls the diffusion coefficient (D), which affects the rate of biomarker transport to the electrodes.^[74]

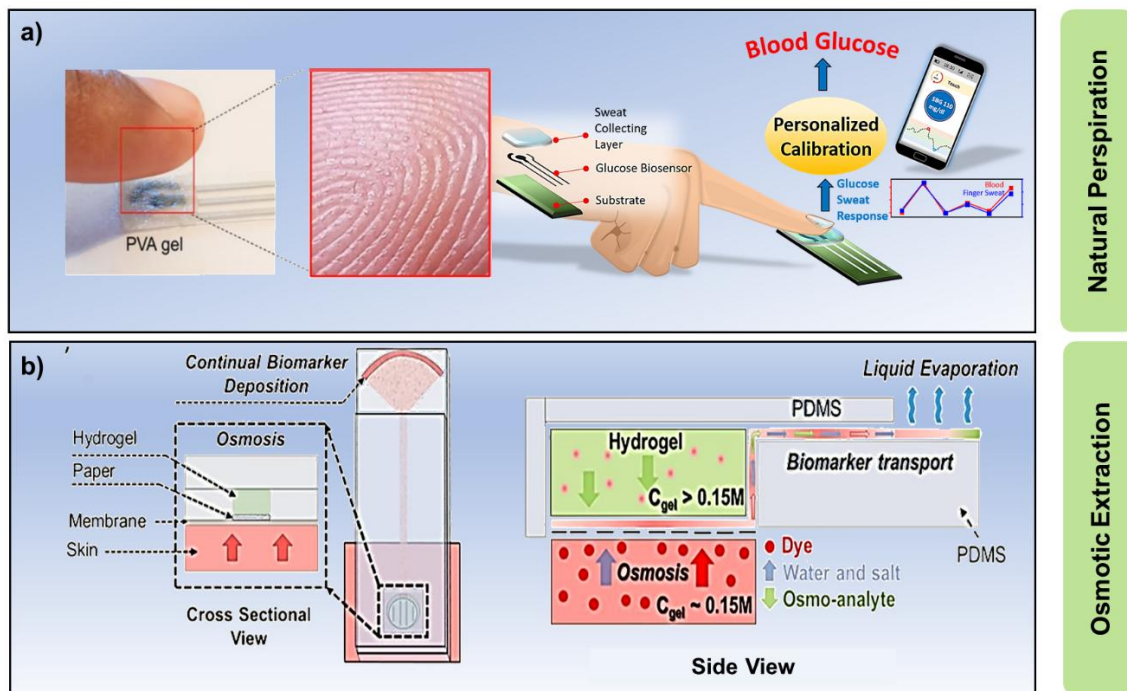


Figure 4: Passive sweat withdrawal techniques. Sweat can be generated on the skin surface without exertion using two ways: (a) Relying on the high natural perspiration rate at fingertips.

The produced sweat can be sampled and transferred to the electrode for sensing using hydrogels.^[43] Adapted with permission. Copyright 2021, American Chemical Society (b) By creating an osmotic pressure difference with respect to sweat inside the skin surface.^[13] This technique can also be deployed with a hydrogel and be combined with evaporation for facilitating long-term collection and sensing. Reproduced with permission. Copyright 2021, American Chemical Society

Another attractive sweat generation via passive sweating involves osmosis, capillary wicking, and evaporation.^[13,23] The prototype shown in **Figure 4b left** executed these principles in a wearable prototype. Osmosis, capillary wicking, and evaporation facilitate simultaneous pumping, transport, and management of sweat, respectively. A polyacrylamide hydrogel equilibrated in a highly concentrated solution of glucose was used to initiate a chemical potential difference with respect to sweat upon interfacing with the skin. A paper microfluidic channel sandwiched between the hydrogel and skin, was used to transport the sampled sweat via capillary action. Furthermore, the end of the paper channel was expanded to a circular fan shaped pad to allow sweat evaporation (**Figure 4b left and right**). Continuous evaporation maintained the capillary pressure in the channel which allowed continuous inflow of sweat from the hydrogel towards the circular pad.^[22] Hence, the evaporation pad acts as a reservoir for all the sweat biomarkers. The prototype would cease to operate if either the chemical potential difference between the sweat and skin nullifies or the evaporation pad gets completely saturated due to solute deposition, allowing no further free space for evaporation. The reported prototype has been used to estimate sweat lactate concentration during rest and under different gradients of exercise^[13], which proved that sweat lactate concentration increases with exercise. Blood lactate concentration and sweat rate were also measured, which showed that the sweat lactate concentration depends on sweat rate and correlates well with blood lactate concentration only under high intensity exercise (70-80% maximum heart rate).^[46,47] Enzymatic based electrochemical sensors based on PB mediated carbon electrodes have also been integrated with this prototype.^[23,48] However, in comparison to the hydrogel-based finger touch-based sensors, this system possesses the following advantages: (a) The hydrogel stays concealed inside a silicone chamber which prevents it from drying; (b) Sweat rate estimation and long-term operation is possible due to continuous sweat evaporation; (c) Osmosis is a colligative property, which means that it only depends on the solute-solvent concentration difference between two mediums.

Overall, although finger touch-based sensing and osmotic hydrogel-based techniques allow painless, non-invasive detection, they result in low sweat volume generation, in comparison to their active sweating technique counterparts. Moreover, the osmotic based technique is also humidity dependent since the evaporation rate depends on it. Hence, all sweat generation mechanisms possess their own advantages and disadvantages. The next section will discuss about the various sweat management techniques.

3. Sweat Management Techniques from Skin

Once the sweat is on the skin surface, it is important to manage it efficiently using appropriate measures to avoid contamination or mixing and support prolonged sensing by delaying the saturation of both the sensor and the sampling substrate.^[52] **Figure 5** highlights the different sweat management techniques reported till date to support long-term sampling and sensing in wearable prototypes. In general, it is relatively difficult to manage the sweat in prototypes that directly interface the skin for sensing, since they can be susceptible to errors arising from either uncontrolled sweat evaporation, dilution, and contamination. Hence, a sampling media is necessary to eliminate the effects of such parameters.

One of the most common and efficient ways of sampling and managing sweat is by using microfluidic channels. The use of microfluidics technologies for biosensing applications has existed since the early 2000's.^[60,75,76] However, it entered the domain of wearable sweat sensing only around the late 2010's^[6-8,77,78], and since then this field has been growing ever since. Microfluidic technologies are good candidates for sweat management since they require smaller sample volumes, allow better control of biomarkers due to the laminar flow, and allow room for integrating automation to reduce human intervention. They can be based on either polymer (PDMS/PMMA)^[8,19], paper^[13], or thread^[20], in which the sensors can be either directly placed inside the channel (common in colorimetric sensors)^[31,49,79,80] or be interfaced to the microfluidic pathway (as in electrochemical platforms).^[6,23,45,81,82] The time lag between introduction of sweat in the channel and its arrival to the sensor is governed by the Taylor-Aris dispersion model.^[83] **Figure 5a** shows an example of a sweat sensing microfluid patch, highlighting the front and backside of a wearable glucose sensing platform that withdraws sweat using IP and samples it in a PDMS microfluidic channel, having electrochemical sensors interfaced to it.^[41] IP was achieved using pilocarpine infused hydrogels, while the sensor relied on a PB mediated gold electrode. The

microfluidic reservoir took ~ 15 mins to get filled up with sweat and the prototype was validated on body for continuous glucose estimation for 20 mins. However, this just represents one example, but apart from this, sweat rate^[54,81,84], metabolites^[13,41,57], electrolytes^[85,86], and nutrition biomarkers^[18,39] – all have been estimated with microfluidic prototypes.

Although microfluidic channels are efficient in sweat handling, they can still experience biofouling from unregulated sweat flow. One such way to prevent this could be via capillary bursting valve (CBV) installation inside the microfluidic channels. This idea was pioneered and deployed in wearable sweat based microfluidic platforms in 2017.^[7,49] CBVs are micron sized features constructed inside microchannels that operate based on the capillary pressure (also referred as “bursting pressure (BP)” in this context) of the fluid. They are mainly used to control flow and even connect microchannels of varying diameters and surface properties.^[87] Each CBV can be designed to accommodate a certain level of BP to allow sequential sweat flow in the channels. The BP depends on the surface tension of the fluid, pressure of the non-wet gaseous phase in the channel, fluid contact angle, and channel dimensions. Channels with a lower width and height would require a greater BP. **Figure 5b** shows a section from a soft, epidermal microfluidic patch consisting of microchambers for sweat storage, each connected with multiple CBVs.^[7] It can be seen that by tuning the BP in each CBV, sweat (herein blue dye solution) can be sequentially guided through multiple channels and microchambers. The fluid inside these microchambers can be also transferred by centrifugation to different collection chambers for biomarker analysis. The resulting prototype was used to estimate sweat lactate and electrolyte levels in each microchamber from actively perspired sweat via colorimetry. This similar concept has been executed in several other sweat microfluidic prototypes.^[21,39,88]

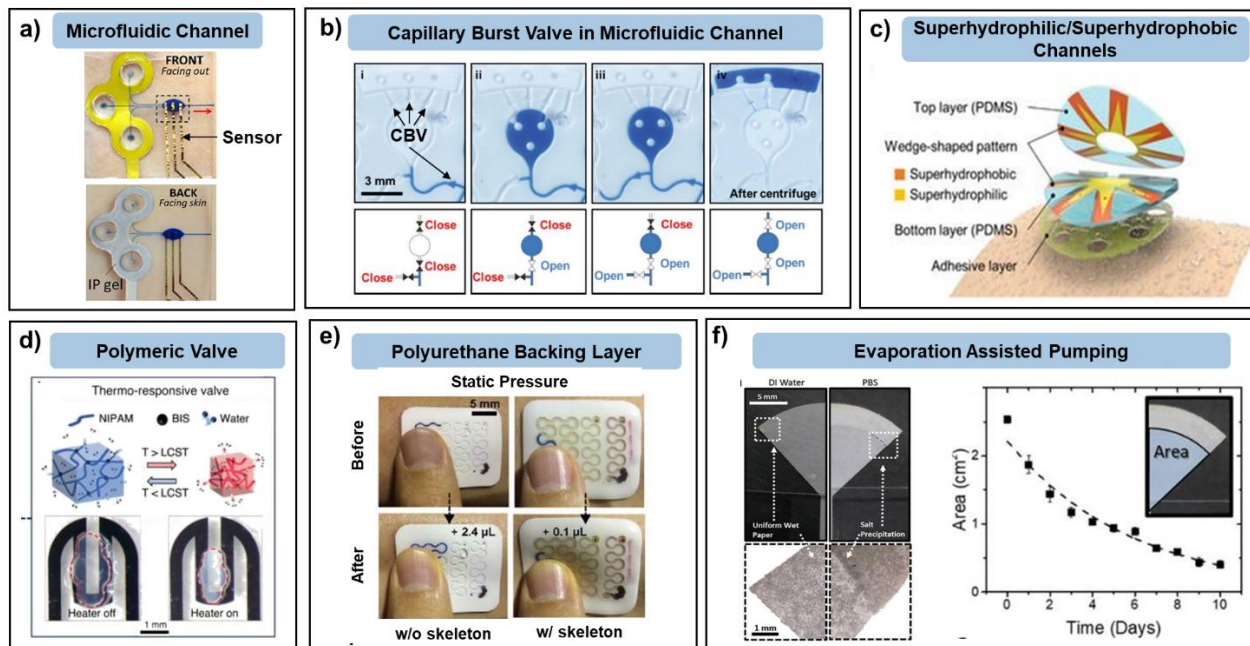


Figure 5: Sweat management techniques in wearable prototypes. (a) Sweat being sampled in microfluidic channels for better biomarker handling.^[41] Adapted with permission. Copyright 2022, Springer-Verlag GmbH Germany, part of Springer Nature (b) Capillary bursting valves installation in microfluidic channels for flow manipulation.^[7] Adapted with permission. Copyright 2017, WILEY-VCH Verlag GmbH & Co. KGaA, Weinheim (c) Superhydrophilic and superhydrophobic coating enabled microfluid pathway.^[89] Reproduced with permission. Copyright 2021, WILEY-VCH Verlag GmbH & Co. KGaA, Weinheim (d) Flow regulation achieved with thermo-responsive polymeric flow valves.^[90] Reproduced with permission. Copyright 2020, Springer-Verlag GmbH Germany, part of Springer Nature (e) External protective polymeric layer over microfluidic platform.^[91] Reprinted with permission. Copyright 2020, Wiley-VCH GmbH (f) Evaporation assisted pumping of sweat using paper microfluidic channels.^[22] Reproduced with permission. Copyright 2020, American Institute of Physics.

The morphology of the substrate and the contact angle between sweat and the substrate can also play an important role towards sweat management.^[92] Inspired by the wedge like shape of a cactus spine, researchers have developed microfluidic channels with both superhydrophilic and superhydrophobic layers, that mimic the shape of such natural structures for managing sweat flow. The PDMS microfluidic prototype shown in **Figure 5c** utilizes this concept.^[89] The superhydrophilic and superhydrophobic layers were created using PVA/silica nanoparticle solution and octadecyltrichlorosilane (ODTS) treatment, respectively, on the channel. This induced variation in the surface morphology of the channel and generated a wettability gradient, which eventually propelled the sweat droplet towards the wide superhydrophilic surface (along the

direction of Laplace pressure). The prototype had electrochemical sensors embedded in the microfluidic pathway, which were used to estimate sweat glucose (with food intake) and lactate concentration (with exercise). This similar concept has also been executed in microwells to develop wearable bandages for multiple sweat biomarker (glucose, chloride, calcium, and pH) sensing.^[18]

External polymeric valves have also been used to regulate the sweat flow in microfluidic channels. The effectivity of such valves remains dependent on external stimulus such as a change in temperature^[90] or moisture.^[53] The prototype reported in **Figure 5d** used a Poly (N-isopropylacrylamide) (PNIPAM) hydrogel as an embedded thermo-responsive valve for flow regulation inside the microfluidic channel.^[90] When the hydrogel temperature crosses lower critical solution temperature (LCST), it allows sweat to flow in the channel. The flow stops when the temperature reaches below LCST. Electrochemical glucose and lactate sensors were also directly interfaced to the microchannel, which measured data from on-body during active perspiration. The whole platform could also be connected to a flexible PCB for wireless data transfer, storage, and monitoring. Moisture dependent polymeric vales have been developed using super absorbent polymers (SAP) such as sodium polyacrylate.^[53] Such materials swell upon water intake and manipulate the flow inside microfluidic channels. Simple touch-based pressure sensitive check valves also exist for sweat flow regulation in microfluidic channels.^[93,94]

Moreover, to prevent the effects of external stresses, polymeric layers have been found to be useful encapsulations for microfluidic prototypes. The prototype reported in **Figure 5e** used an external polyurethane (PU) skeleton layer for this purpose.^[91] PU was chosen because of its high modulus (~ 1.1 GPa). The rigid layer made the prototype be resistive to external compression, impacts, acceleration, and evaporation, and allowed successful colorimetric sweat chloride detection under these conditions. Similarly, another wearable microfluidic prototype was developed using hydrophobic poly(styrene-isoprene-styrene), that not only made it stress resistive, but also be resistive to external moisture.^[55]

Apart from the conventional polymer-based microfluidic channels, paper can be also used as an effective substrate for sampling, transporting, and managing sweat. We have already discussed in **Figure 4b** how paper microfluidic channels can be utilized under passive sweating. Paper is not only inexpensive, thin, and widely available, but its porous nature and ability to control

flow rates via capillary wicking and evaporation, makes it a suitable medium for sweat management.^[95,96] Evaporation assisted pumping in microfluidic channels has existed for quite a while.^[97-99] However, the first study to show that this concept can also be used for sweat pumping was reported recently and is shown in **Figure 5f**.^[22] Such paper channel design consisted of a rectangular section and an evaporation pad of large surface area. As sweat enters the pad, it starts to evaporate and leaves behind solute deposition. Evaporation maintains the capillary pressure in the channel (by preventing it from complete wetting) which facilitates long-term sweat inflow by delaying saturation. *In-vitro* studies have shown that by carefully tuning the width, length of the rectangular channel, and pad area, continuous flow can be sustained for up to ~ 10 days. With time, the rate of sweat evaporation from the pad would decrease due to continuous solute deposition (lack of free space for evaporation). Overall, the evaporation pad can also act as a repository for all sweat biomarkers and can be used for *ex-situ* sensing. This study laid the foundation for the design of the osmotic wearable prototype reported in **Figure 4b**. The next section will discuss the future directions and prospects, with a focus on the high-tech and advanced applications of sweat sensing in general.

4. New Directions for Sweat Sensing

Till now, we have seen how sweat can be sampled, accessed on the skin surface, and be managed using different tools and techniques for prolonged collection/sensing through delayed saturation in wearable prototypes. Considering all those aspects, the field of sweat sensing has witnessed considerable development in the past few years, with prototypes majorly focusing on long-term monitoring (~ hours), wireless real-time data monitoring on smart devices, multiplexing with other biomarkers, energy harvesting through BFCs, integration with physiological signal monitoring, and utilizing them for high-tech real-world applications. Hence, we will focus on all these aspects in this section and discuss them based on the sequential integration of multiple aspects to sweat sensors towards next generation and advanced applications.

The usage of smart devices (computers, laptops, mobile phones, tablets) for monitoring and storing the real-time biomarker signals, as obtained from the wearable sensors have expanded widely. Amongst these, smartphones have proven to be the most useful tool for such purposes since they are portable, have become affordable to the general population, and have in built features that allow storage and sharing of data. In today's world, smartphone assisted monitoring

is being allowed by all the leading commercial health and fitness monitoring devices, such as Apple Watch or Fitbits, and continuous glucose monitors (CGMs) of Abbott or Dexcom. Furthermore, smartphones also allow the users to share their health data with and receive assistance from their healthcare providers, eventually preventing them from cumbersome in-person doctor visits.

The rapid growth of smartphone usage has also made it enter the field of sweat sensing. The utilization of smartphone highly depends upon the sensing mechanism of the wearable prototype. In colorimetric microfluidic sensors, the concentration of the biomarker is predicted by estimating the color intensity of the generated compound, post reaction with the assay, using image analysis techniques.^[8,10,31,80,84,100,101] The prototype shown in **Figure 6a** uses this concept for sweat rate and chloride estimation for sport science applications.^[84] The prototype consists of PDMS microfluidic channels with an embedded colorimetric chloride assay. By mapping the color intensity of the generated compound (upon the interaction of sweat chloride with the assay) using computer vision algorithms, the dynamic sweat rate and chloride content were estimated. The prototype was tested on 312 subjects from which a good correlation between sweat chloride concentration and sweat rate was observed. Advanced machine learning based algorithms have also been deployed with this prototype recently for further accurate estimations of sweat rate and chloride concentration.^[102] Alternatively, smartphone-based monitoring can be achieved with electrochemical platforms by connecting them to circuit boards having in built electronic modules for allowing wireless data transmission (via Bluetooth) and storage.^[4,23,65]

The use of laser engraving for fabricating both microfluidic channels and sensor has received a considerable recent attention.^[5,57] The traditional approaches for fabricating silicone based microfluidic channels are expensive, time consuming, and not scalable.^[4,8] Hence, CO₂ based laser engraving techniques have gained recognition since they allow rapid fabrication of different patterns under ambient conditions, which allow scalable production of wearable sensors within less time.^[5,103] Electrodes can also be fabricated using lasers. Laser induced graphene (LIG) is produced by scribing infrared (IR) laser on a polyimide (PI) substrate which photothermally converts the carbon atoms from sp³ to sp² orientation. As a result, the C-O, C=O, and N=C bonds in the PI get broken, generating porous graphene nanosheets with more than 85% carbon content.^[104] Hence, LIG electrodes provide high surface-to-volume ratio due to enhanced porosity

in comparison to traditional graphene.^[105] The prototype shown in **Figure 6b** followed these principles and was used to detect uric acid (UA) and tyrosine in sweat^[5], where the LIG-based sensors could measure up to 200 μM and 1000 μM of uric acid and tyrosine, respectively. The prototype could monitor temperature and strain with LIG sensors, and was even validated on gout patients, where their UA concentration ranged $\sim 80\text{-}160$ μM . Another prototype based on the similar concept was also developed for sweat cortisol sensing for tracking the circadian rhythm of the human body.^[57]

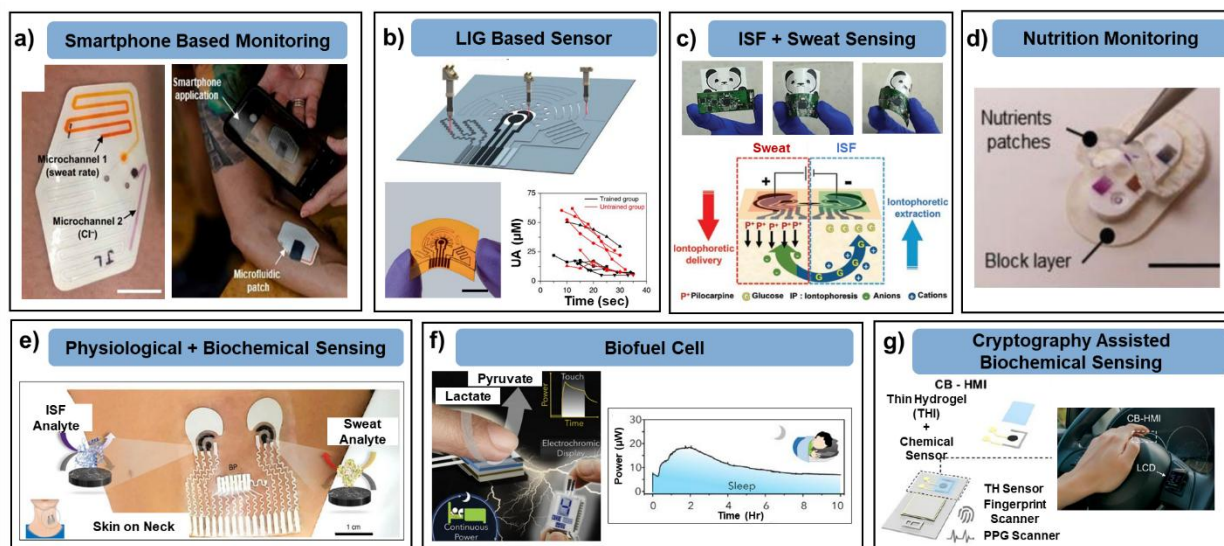


Figure 6: Recent advancements in the field of sweat sensing. (a) Smartphone based detection for estimating sweat biomarker levels. Reproduced with permission.^[84] Copyright 2020, American Association for the Advancement of Science. (b) Usage of laser for engraving microfluidic channels and porous electrode fabrication.^[5] Reproduced with permission. Copyright 2019, Springer Nature. (c) Simultaneous monitoring of multiple biomarkers from multiple biofluids on a single wearable platform.^[40] Reproduced with permission. Copyright 2018, WILEY-VCH Verlag GmbH & Co. KGaA, Weinheim (d) Sweat nutrition biomarker monitoring platform.^[39] Reproduced with permission. Copyright 2021, WILEY-VCH Verlag GmbH & Co. KGaA, Weinheim. (e) Hybrid wearable patch comprising both biophysical and biochemical monitoring systems.^[106] Reprinted with permission. Copyright 2021, Springer Nature. (f) Biofuel cell based long-term energy harvesting from sedentary subjects.^[26] Reprinted with permission. Copyright 2021 Elsevier Inc. (g) Biochemical signal-machine interfacing systems for encrypted data storage and feedback-based systems.^[107] Reprinted with permission. Copyright 2022, National Academy of Science.

Researchers have also tried to simultaneously target the sensing of two different biomarkers from two different biofluids using a single wearable platform. The prototype shown in

Figure 6c was developed on a tattoo paper which used IP to simultaneously withdraw sweat and ISF for sensing alcohol and glucose, respectively.^[40] IP was applied through transdermal pilocarpine delivery from the anodic electrode terminal, which triggered an electroosmotic flow inside the skin. This led to the flow of sweat and cations towards the anode, and ISF and glucose towards the cathode (along the direction of electroosmotic flow). Hence, alcohol and glucose sensors were placed at the anode and cathode, respectively. On-body testing (with meal and 5-12 oz of alcoholic beverage) with 5 mins of IP showed glucose and alcohol response, which also correlated with their concentration in blood.

Nutrition biomarkers have also started to get a lot of attention recently due to their link with disease management and functioning of the immune system.^[108] Inadequate nutrition status can prove catastrophic in terms of affecting ones physical, and mental health and also be responsible towards chronic disease development.^[109] Vitamins (A, B6, B12,C, D3, and E)^[110], minerals (Zn, Fe)^[111], Ca^{2+} ^[118], Mg^{2+} ^[32], β -hydroxybutyrate (BHB)^[112], and cholesterol^[113] are some of the important nutritional biomarkers that have been monitored from different human biofluids. Although there has been a good progress in terms of sensing these biomarkers on benchtop settings, only a few sweat based wearable platforms have been reported.^[9,39,66] One of the recently developed prototype is shown in **Figure 6d**, which was designed to simultaneously transdermally deliver and monitor vitamin C, Zn, Fe, and Ca^{2+} , using colorimetry.^[39] The platform consisted of PDMS microfluidic channels which had the specific assays embedded in them. The sensors could estimate up to 100 μM , 100 μM , 100 μM , and 3 mM of vitamin C, Zn, Fe, and Ca^{2+} , respectively. During on body validation, the nutrients were first delivered transdermally through the skin and then monitored in sweat generated through sauna. A good correlation was also observed with their levels in blood. Moreover, IP stimulated sweat has also been used for monitoring nutrition biomarkers (amino acids, vitamins, and BHB), using MIPs^[66] and simple enzymatic sensors.^[9]

Continuous monitoring of biophysical signals (such as blood pressure (BP) and heart rate (HR)) also play a significant role in determining the physiological condition of the human body. Hence, their monitoring is as important as the monitoring of biochemical signals. A prototype capable of measuring simultaneously these biochemical and biophysical signals could prove extremely useful for monitoring severe health conditions such as obesity, diabetes, and

cardiovascular diseases. The first wearable prototype to execute this functionality was reported in 2016,^[38] where only sweat lactate and HR were monitored under active sweating. However, the prototype shown in **Figure 6e** was the first one to extend this functionality towards multiplexed sensing from different biofluids in a single wearable form factor.^[106] The prototype was developed on a conformal, stretchable substrate using styrene-ethylene-butylene-styrene (SEBS) elastomer, which could simultaneously monitor glucose, lactate, caffeine and alcohol enzymatically, while BP and HR using ultrasonic transducers. The transducers were developed using lead zirconate titanate (PZT), with glucose being targeted from ISF, caffeine and alcohol from IP stimulated sweat, and lactate from actively perspired sweat.

Despite the tremendous progress towards sweat based wearables, the amount of power consumed during sensing remains a potential issue. Most of the wearable prototypes are powered either by a commercial Li-ion battery (which can be bulky and heavy) or near field communication (NFC) chips. Additionally, if the prototype runs on IP, the power consumption increases further (as high as ~ 30 mW for IP and 6 mW for sensing).^[40] Although with passive sweat collection the power consumption reduces significantly^[23], the problem still remains unsolved for prototypes running on active perspiration. These shortcomings have led to the development of wearable sweat based BFC for harvesting power.^[114,115] Sweat based BFC's use lactate as a fuel since it can be generated easily with exertion and its concentration range in sweat is high (~ mM). The enzymatic lactate bioelectrode served as the anode for catalyzing the oxidation of lactate to pyruvate, while the cathode undergoes a reduction reaction in presence of either bilirubin oxidase enzyme (BOx)^[27], Pt^[115], or Ag₂O.^[116] Sweat based BFCs have been able to achieve power density as high as ~ 1.2 mW/cm², being capable enough to run a light emitting diode (LED) and Bluetooth low energy (BLE) radio.^[116] Additionally, power harvested by BFCs have also been stored in supercapacitors.^[117,118]

Although sweat based BFCs have proven to be extremely efficient, a major drawback experienced by them lies in being functional only under active perspiration. Thus, these BFCs would not operate under low humidity conditions or on rested subjects. The prototype shown in **Figure 6f** has addressed this problem by harvesting power from a simple touch of the finger.^[26] Porous PVA hydrogels were used to sample and transport the sweat lactate from the fingertip to the BFC. The BFC was developed using CNT foam with LOx and Pt on the anode and cathode,

respectively. By making the BFCs be in continuous contact for 10 hr on the finger during sleep, $\sim 300 \text{ mJ/cm}^2$ ($\sim 30 \text{ mJ}$ of energy per hour) of power output was obtained. Since a single press on finger consumes $\sim 0.5 \text{ mJ}$ of energy, this whole system resulted in a high energy return on investment (~ 60 times higher). Furthermore, the harvested power was also utilized to operate thermochromic displays for Na^+ and vitamin C sensors.

The concept of touch-based sensing has also been merged with machine encryption to develop a bio-human-machine interface system, which would translate the touch based entries to biochemical and biophysical indices, and eventually store them in cloud memory (**Figure 6g**).^[107] Such interfacing is achieved by executing special algorithms that enable biometric encryption of one's physiological parameters. The prototype reported in **Figure 6g** used a conventional touch-based platform (using hydrogels) to obtain the biochemical signals of alcohol and acetaminophen (Ac) from the fingertip. The enzymatic sensors of alcohol and acetaminophen were designed to measure up to 2.5 mM and $12 \text{ }\mu\text{M}$, respectively *in-vitro*. Biophysical signals such as heart rate and SpO_2 were also measured in conjunction. The whole prototype was even deployed on a steering wheel of a car for *in-vivo* demonstration of alcohol presence in the body. The display screen would instantly show an alert message if sweat alcohol content surpassed the limit. Such a system - if connected to the car ignition system - can eventually restrict drivers from driving under influence (DUI). Furthermore, the Ac platform was even connected to a feedback-based system which would determine the medication requirement of the subject, based on the Ac levels.

5. Conclusions and Outlook

Sweat contains a plethora of biomarkers that coexist in blood and serves as an easily accessible non-invasive biofluid. It is secreted mostly by the eccrine sweat glands, where its accumulation occurs due to osmotic effects between the glands and their surroundings. The continuous transport of sweat onto the epidermis is driven by capillary effects and evaporation. Sweat can be actively generated on the epidermis with physical exertion, chemical stimulation, and/or thermal stimulation, while passively relying on either the resting perspiration rate or osmosis. Furthermore, long-term sweat inflow and extended sensing can be achieved with different microfluidic substrates comprising polymeric valves for flow regulation in the channels, along with tuning the surface morphology of the flow channel, and/or by allowing continuous evaporation. Owing to the sweat management strategies described in this article, the recent advances in sweat sensing

prototypes have marked a transition to smartphone-based extended monitoring with cloud data storage, multiplexed biophysical and biochemical sensor arrays, and even wearable biofuel cells for self-powered multiplexed sweat sensing. **Table 1** highlights the list of all key sweat biomarkers with their reported extraction techniques, correlation with blood, and the diseases linked with their levels in sweat. Overall, understanding the biochemical pathway of such biomarkers and their correlation to blood is subjected to the individual's health and testing conditions, which wearable prototypes have been trying to solve, develop, and improve continuously.

Table 1. Analytes in sweat with their extraction and correlation information with blood.

Analyte	Sweat extraction modality	Concentration:		Correlation/ Validation *	Importance	Ref.
		Sweat	Blood			
Sodium (Na ⁺)	Active	30 - 90 mM [119]	135-150 mM [120]	Y/Y [121,122]	Dehydration, hyponatremia	[4,123]
Chloride (Cl ⁻)	Active	10 -100 mM [119]	96–106 mM [120]	Y/Y [122,124]	Cystic fibrosis, dehydration	[125,126]
Potassium (K ⁺)	Passive	1-24 mM [119]	5-6 mM [127]	Y/Y [121,122]	Ambulatory monitoring, sweat quality control	[30,128]
Calcium (Ca ²⁺)	Active	0-15 mM [129]	1-3 mM [130]	Y/N [131,132]	Metabolism, Homeostasis	[129,132]
Ammonium (NH ₄ ⁺)	Active	0.8 - 8 mM [133]	30-80 μM [127,133]	Y/N [134]	Metabolic conditions	[134,135]
pH	Active	3 - 8 [3]	6.3 - 7.4 [136]	Y/Y [121,122]	Homeostasis dysregulation, stress	[137,138]
Glucose	Active and Passive	10-200 μM [139]	x10-100 times higher [139]	Y/Y [140]	Diabetes	[141,142]
Lactate	Active and Passive	4-100 mM [119]	0.5-15 mM [143]	Y/N [144]	Muscle fatigue, Tissue hypoxia	[145,146]
Ethanol	Passive	2.5-22.5 mM [1]	~2.5-22.5 mM [1]	Y/Y [147,148]	Personal health, Social order	[11,147]
Uric Acid	Passive	18 - 33 μM [149]	5-7 mM [127]	N/N	Chronic nephritis	[150,151]

Ascorbic Acid	Passive	1 - 50 μM [152]	10-200 μM [152]	Y/N [132]	Arthritis, Parkinson's, Alzheimer's, cardiovascular disease, cancer	[123,132,150]
Cortisol	Passive	8 - 150 ng/ml [153]	2-25 $\mu\text{g/ml}$ [154]	Y/Y [154]	Mental diseases, fatigue, stress	[155,156]
Caffeine	Passive	0-5 $\mu\text{g/mL}$ [157]	0-30 μM [157]	Y/Y [106]	Performance	[42,158]
Neuropeptide Y	Passive	0.8 - 75 pg/mL [159]	0.5 - 70 pg/mL [159]	Y/Y [160]	Depression, stress	[123,161]
Levodopa (L- dopa)	Passive	0 - 2.5 μM [162]	0-9 $\mu\text{g/mL}$ [163]	Y/N [164]	Tardive dyskinesia	[44,164,165]
MicroRNAs	Active	-	-	N/N [166]	Regulation of biological processes	[166]

*Y: Yes, N: No

Despite these advancements, there remains certain challenges that require attention. These challenges are highlighted below:

- A. Not all wearable sweat sensing platforms have an integrated system built for estimating sweat rate. Quantifying the real-time sweat generation rate is important to understand the dependency of the biomarker amount on the volume of sweat produced. The prototypes quantifying sweat rate are mostly impedimetric, that are sensitive to the total ionic content of sweat. Hence, most of the platforms measuring non-ionic biomarker levels either do not measure sweat rate or rely on the visual progression (like tracking a dye trace in a microfluidic channel) of sweat. Sweat rate estimation via visual progression is a qualitative approach. Although recent studies have validated such methods on a large pool of subjects, quantified its performance with integrated mobile-based imaging tools, and compared its efficiency with respect to absorption pads (gold standard technique), they remain executable only on microfluidic channels with actively perspired sweat.^[84] Moreover, there are only a few platforms that discuss sweat rate when measuring on sedentary individuals and its effect on the concentration of a few target molecules (glucose, cytokines, and cortisol).^[32] Hence, a universal sweat rate estimation technique remains to be engineered.

- B. Most reported BFC patches operate solely on sweat lactate. Lactate is an oxidative stress biomarker which increases in sweat with physical exertion. Moreover, excessive exertion can dilute the sweat lactate concentration and even force the unhealthy subjects to cross their lactate threshold (appearance of lactate in blood), eventually proving detrimental for them.^[167] Although BFC operation has been demonstrated using sweat lactate from resting subjects, the process still remains time-consuming due to the low perspiration rate. Furthermore, the biochemical partitioning of many sweat metabolites remains inadequately understood. Hence, more comprehensive studies focused on addressing these constraints are required, instead of simply developing a sensor that expands the pool of measurable sweat-borne metabolites. Upon further progress, these new sweat-borne metabolites should also be investigated for BFC applications, since power consumption is a major constraint dictating the feasibility and functionality of wearable sensors/electronics.
- C. Proteins, DNA, neuropeptides, and cytokines hold huge potential in determining the health condition of an individual since they are sensitive indicators of disease and inflammation. However, since these biomarkers are present in extremely diluted levels in sweat (~ ng/mL or pg/mL), further research efforts are needed to develop ultrasensitive sensors targeting such trace biomarkers.
- D. There also remains a lack of closed loop feedback-based drug delivery systems coupled with sweat sensing prototypes. In such systems, whenever the measured biomarker concentration value would exceed its normal level, a tuned dose of the drug would be released into the body to counter the detrimental effects of the disease biomarker. The foremost constraints of such sense-act-treat systems would be the variable dilution of the analyte depending on the varying sweat generation rate of the individual, inadequate precision in timed release of the drug owing to the time offset between sweat versus blood-based biomarker profiles, as well as the possible non-internalization/inefficient drug uptake through the skin because of the sweat flow rate and/or skin conductivity, among other subjective physiological parameters. However, with further progress on addressing these uncertainties, the development of such closed-loop technologies for addressing multiple disease biomarkers would contribute strongly towards the development of at-home

personalized healthcare, bearing unique physiological and user-related benefits of its noninvasive approach.

E. The commercialization of current wearable sweat sensors requires further attention to several issues. Such issues are attributed to the following two reasons: (a) Most fully integrated, wearable sweat sensors can only estimate the biomarker levels with biochemical sensors. However, if one wants to gain necessary health information from sweat, decisions should be made by simultaneously monitoring both biochemical and biophysical signals (heart rate, pulse, SpO₂, core body temperature, blood pressure). Although, a multiplexed platform capable of such multi-modal operation has been recently reported^[106], there still remains room for improvement and great need for more of such platforms with extensive on-body validation. (b) Biochemical sensors rely on enzymes for operation. Many enzymes are fragile and their activity depends on the biofluid temperature and pH. Hence, highly stable non-enzymatic synthetic receptors sensing ways (using nanozymes,^[168,169] or MIPs^[66]) need to be explored. Furthermore, inclusion of evaporation to microfluidic prototypes can prevent them from biofouling and sustain long-term, continuous wearable performance. (c) Most wearable prototypes show the sensor operation on-body without validation against gold standard analytical techniques (e.g., high performance liquid chromatography (HPLC), mass spectroscopy). Such large-scale validations are necessary to assess their accuracy and understand their operation and performance under varying physiological conditions.

Overall, the field of sweat sensing still has a long way to go in terms of understanding the biochemical partitioning of several biomarkers, development of a universal sweat rate estimation technique, and understanding the correlation of sweat-borne biomarker levels with disease onset and progression through extensive clinical trials and pilot studies. Till date, only one conventional microfluidic based wearable sweat sensor (for sweat rate, Na⁺, and Cl⁻ detection) has been commercialized post intense clinical validation.^[84] Hence, there remains a pressing need for the development of novel sweat-management and sensing platforms, multifunctional sweat-powered autonomous wearables, and most importantly, comprehensive study protocols targeting these pitfalls in sweat analysis.

Acknowledgement

Tamoghna Saha and Rafael Del Caño contributed equally to this work. J.W. acknowledges support from the UCSD Center of Wearable Sensors (CWS). R.D.C. acknowledges support from “*Plan Propio de Investigación de la Universidad de Córdoba 2021*”.

Conflict of Interest

The authors declare no conflicts of interest.

References

- [1] Z. Sonner, E. Wilder, J. Heikenfeld, G. Kasting, F. Beyette, D. Swaile, F. Sherman, J. Joyce, J. Hagen, N. Kelley-Loughnane, R. Naik, *Biomechanics* **2015**, 9, 031301.
- [2] L. B. Baker, *Temperature* **2019**, 6, 211.

- [3] M. Bariya, H. Y. Y. Nyein, A. Javey, *Nat. Electron.* **2018**, *1*, 160.
- [4] W. Gao, S. Emaminejad, H. Y. Y. Nyein, S. Challa, K. Chen, A. Peck, H. M. Fahad, H. Ota, H. Shiraki, D. Kiriya, D.-H. Lien, G. A. Brooks, R. W. Davis, A. Javey, *Nature* **2016**, *529*, 509.
- [5] Y. Yang, Y. Song, X. Bo, J. Min, O. S. Pak, L. Zhu, M. Wang, J. Tu, A. Kogan, H. Zhang, T. K. Hsiai, Z. Li, W. Gao, *Nat. Biotechnol.* **2020**, *38*, 217.
- [6] A. Martín, J. Kim, J. F. Kurniawan, J. R. Sempionatto, J. R. Moreto, G. Tang, A. S. Campbell, A. Shin, M. Y. Lee, X. Liu, J. Wang, *ACS Sensors* **2017**, *2*, 1860.
- [7] J. Choi, D. Kang, S. Han, S. B. Kim, J. A. Rogers, *Adv. Healthc. Mater.* **2017**, *6*, (5).
- [8] A. Koh, D. Kang, Y. Xue, S. Lee, R. M. Pielak, J. Kim, T. Hwang, S. Min, A. Banks, P. Bastien, M. C. Manco, L. Wang, K. R. Ammann, K.-I. Jang, P. Won, S. Han, R. Ghaffari, U. Paik, M. J. Slepian, G. Balooch, Y. Huang, J. A. Rogers, *Sci. Transl. Med.* **2016**, *8*, 366ra165.
- [9] J. R. Sempionatto, A. A. Khorshed, A. Ahmed, A. N. De Loyola E Silva, A. Barfidokht, L. Yin, K. Y. Goud, M. A. Mohamed, E. Bailey, J. May, C. Aebischer, C. Chatelle, J. Wang, *ACS Sensors* **2020**, *5*, 1804.
- [10] Y. Zhang, H. Guo, S. B. Kim, Y. Wu, D. Ostojich, S. H. Park, X. Wang, Z. Weng, R. Li, A. J. Bandonkar, Y. Sekine, J. Choi, S. Xu, S. Quaggin, R. Ghaffari, J. A. Rogers, *Lab Chip* **2019**, *19*, 1545.
- [11] J. Kim, I. Jeerapan, S. Imani, T. N. Cho, A. Bandonkar, S. Cinti, P. P. Mercier, J. Wang, *ACS Sensors* **2016**, *1*, 1011.
- [12] T. Shay, M. D. Dickey, O. D. Velev, *Lab Chip* **2017**, *17*, 710.
- [13] T. Saha, J. Fang, S. Mukherjee, M. D. Dickey, O. D. Velev, *ACS Appl. Mater. Interfaces* **2021**, *13*, 8071.
- [14] K. Nagamine, T. Mano, A. Nomura, Y. Ichimura, R. Izawa, H. Furusawa, H. Matsui, D. Kumaki, S. Tokito, *Sci. Rep.* **2019**, *9*, 1.
- [15] C. J. Smith, G. Havenith, *Eur. J. Appl. Physiol.* **2011**, *111*, 1391.

- [16] M. Phillips, R. E. Vandervoort, C. E. Becker, *J. Invest. Dermatol.* **1977**, 68, 221.
- [17] A. Lynch, D. Diamond, M. Leader, *Analyst* **2000**, 125, 2264.
- [18] X. He, T. Xu, Z. Gu, W. Gao, L. P. Xu, T. Pan, X. Zhang, *Anal. Chem.* **2019**, 91, 4296.
- [19] A. Martín, J. Kim, J. F. Kurniawan, J. R. Sempionatto, J. R. Moreto, G. Tang, A. S. Campbell, A. Shin, M. Y. Lee, X. Liu, J. Wang, *ACS Sensors* **2017**, 2, 1860.
- [20] G. Xiao, J. He, Y. Qiao, F. Wang, Q. Xia, X. Wang, L. Yu, Z. Lu, C.-M. Li, *Adv. Fiber Mater.* **2020**, 2, 265.
- [21] J. Choi, A. J. Bandodkar, J. T. Reeder, T. R. Ray, A. Turnquist, S. B. Kim, N. Nyberg, A. Hourlier-Fargette, J. B. Model, A. J. Aranyosi, S. Xu, R. Ghaffari, J. A. Rogers, *ACS Sensors* **2019**, 4, 379.
- [22] T. Shay, T. Saha, M. D. Dickey, O. D. Velev, *Biomicrofluidics* **2020**, 14, 034112.
- [23] T. Saha, T. Songkakul, C. T. Knisely, M. A. Yokus, M. A. Daniele, M. D. Dickey, A. Bozkurt, O. D. Velev, *ACS Sensors* **2022**, 7, 2037.
- [24] X. He, C. Fan, T. Xu, X. Zhang, *Nano Lett.* **2021**, 21, 8880.
- [25] L. Wang, T. Xu, X. He, X. Zhang, *J. Mater. Chem. C* **2021**, 9, 14938.
- [26] L. Yin, J. Moon, R. Sempionatto, ~~S. Xu, J. Wang, L. Yin, J. Moon, J. R. Sempionatto~~, M. Lin, M. Cao, A. Trifonov, F. Zhang, Z. Lou, J. Jeong, S. Lee, S. Xu, [J. Wang](#), *Joule* **2021**, 5, 1888.
- [27] X. Chen, L. Yin, J. Lv, A. J. Gross, M. Le, N. G. Gutierrez, Y. Li, I. Jeerapan, F. Giroud, A. Berezovska, R. K. O. Reilly, S. Xu, S. Cosnier, J. Wang, R. K. O'Reilly, S. Xu, S. Cosnier, J. Wang, *Adv. Funct. Mater.* **2019**, 29, 1.
- [28] S. Lin, B. Wang, Y. Zhao, R. Shih, X. Cheng, W. Yu, H. Hojaiji, H. Lin, C. Hoffman, D. Ly, J. Tan, Y. Chen, D. Di Carlo, C. Milla, S. Emaminejad, *ACS Sensors* **2020**, 5, 93.
- [29] B. Schazmann, D. Morris, C. Slater, S. Beirne, C. Fay, R. Reuveny, N. Moyna, D. Diamond, *Anal. Methods* **2010**, 2, 342.
- [30] S. Emaminejad, W. Gao, E. Wu, Z. A. Davies, H. Yin Yin Nyein, S. Challa, S. P. Ryan,

- H. M. Fahad, K. Chen, Z. Shahpar, S. Talebi, C. Milla, A. Javey, R. W. Davis, *Proc. Natl. Acad. Sci.* **2017**, *114*, 4625.
- [31] T. R. Ray, M. Ivanovic, P. M. Curtis, D. Franklin, K. Guventurk, W. J. Jeang, J. Chafetz, H. Gaertner, G. Young, S. Rebollo, J. B. Model, S. P. Lee, J. Ciraldo, J. T. Reeder, A. Hourlier-Fargette, A. J. Bandodkar, J. Choi, A. J. Aranyosi, R. Ghaffari, S. A. McColley, S. Haymond, J. A. Rogers, *Sci. Transl. Med.* **2021**, *13*, DOI 10.1126/scitranslmed.abd8109.
- [32] L. B. Baker, A. S. Wolfe, *Physiological Mechanisms Determining Eccrine Sweat Composition*, Springer Berlin Heidelberg, **2020**.
- [33] M. Constantinescu, B. C. Hilman, *Lab. Med.* **1996**, *27*, 472.
- [34] P. Heinonen, A. Iitiä, T. Torresani, T. Lövgren, *Clin. Chem.* **1997**, *43*, 1142.
- [35] M. J. Tierney, J. A. Tamada, R. O. Potts, L. Jovanovic, S. Garg, *Biosens. Bioelectron.* **2001**, *16*, 621.
- [36] W. Gao, S. Emaminejad, H. Y. Y. Nyein, S. Challa, K. Chen, A. Peck, H. M. Fahad, H. Ota, H. Shiraki, D. Kiriya, D. H. Lien, G. A. Brooks, R. W. Davis, A. Javey, *Nat.* **2016**, *529*, 509.
- [37] H. Y. Y. Nyein, W. Gao, Z. Shahpar, S. Emaminejad, S. Challa, K. Chen, H. M. Fahad, L. C. Tai, H. Ota, R. W. Davis, A. Javey, *ACS Nano* **2016**, *10*, 7216.
- [38] S. Imani, A. J. Bandodkar, A. M. V. Mohan, R. Kumar, S. Yu, J. Wang, P. P. Mercier, *Nat. Commun.* **2016**, *7*, 11650.
- [39] J. Kim, Y. Wu, H. Luan, D. S. Yang, D. Cho, S. S. Kwak, S. Liu, H. Ryu, R. Ghaffari, J. A. Rogers, *Adv. Sci.* **2022**, *9*, 1.
- [40] J. Kim, J. R. Sempionatto, S. Imani, M. C. Hartel, A. Barfidokht, G. Tang, A. S. Campbell, P. P. Mercier, J. Wang, *Adv. Sci.* **2018**, *5*, 1800880.
- [41] G. Bolat, E. De la Paz, N. F. Azeredo, M. Kartolo, J. Kim, A. N. de Loyola e Silva, R. Rueda, C. Brown, L. Angnes, J. Wang, J. R. Sempionatto, *Anal. Bioanal. Chem.* **2022**, *414*, 5411.

- [42] W. Tang, L. Yin, J. R. Sempionatto, J. Moon, H. Teymourian, J. Wang, *Adv. Mater.* **2021**, *33*, 2008465.
- [43] J. R. Sempionatto, J.-M. Moon, J. Wang, *ACS Sensors* **2021**, *6*, 1875.
- [44] J. M. Moon, H. Teymourian, E. De la Paz, J. R. Sempionatto, K. Mahato, T. Sonsa-ard, N. Huang, K. Longardner, I. Litvan, J. Wang, *Angew. Chemie - Int. Ed.* **2021**, *60*, 19074.
- [45] H. Y. Y. Nyein, M. Bariya, B. Tran, C. H. Ahn, B. J. Brown, W. Ji, N. Davis, A. Javey, *Nat. Commun.* **2021**, *12*, 1.
- [46] T. Saha, J. Fang, S. Mukherjee, C. T. Knisely, M. D. Dickey, O. D. Velev, *Micromachines* **2021**, *12*, 1513.
- [47] T. Saha, J. Fang, M. A. Yokus, S. Mukherjee, A. Bozkurt, M. A. Daniele, M. D. Dickey, O. D. Velev, in *2021 43rd Annu. Int. Conf. IEEE Eng. Med. Biol. Soc.*, IEEE, **2021**, pp. 6863–6866.
- [48] M. A. Yokus, T. Saha, J. Fang, M. D. Dickey, O. D. Velev, M. A. Daniele, in *2019 IEEE SENSORS*, IEEE, **2019**, pp. 1–4.
- [49] J. Choi, Y. Xue, W. Xia, T. R. Ray, J. T. Reeder, A. J. Bandodkar, D. Kang, S. Xu, Y. Huang, J. A. Rogers, *Lab Chip* **2017**, *17*, 2572.
- [50] W. Jia, A. J. Bandodkar, G. Valdés-Ramírez, J. R. Windmiller, Z. Yang, J. Ramírez, G. Chan, J. Wang, *Anal. Chem.* **2013**, *85*, 6553.
- [51] S. B. Kim, J. Koo, J. Yoon, A. Hourlier-Fargette, B. Lee, S. Chen, S. Jo, J. Choi, Y. S. Oh, G. Lee, S. M. Won, A. J. Aranyosi, S. P. Lee, J. B. Model, P. V. Braun, R. Ghaffari, C. Park, J. A. Rogers, *Lab Chip* **2020**, *20*, 84.
- [52] C. Liu, T. Xu, D. Wang, X. Zhang, *Talanta* **2020**, *212*, 120801.
- [53] S. Soft, S. B. Kim, Y. Zhang, S. M. Won, A. J. Bandodkar, Y. Sekine, Y. Xue, J. Koo, S. W. Harshman, J. A. Martin, J. M. Park, T. R. Ray, K. E. Crawford, K. Lee, J. Choi, R. L. Pitsch, C. C. Grigsby, A. J. Strang, Y. Chen, S. Xu, J. Kim, A. Koh, J. S. Ha, Y. Huang, S. W. Kim, J. A. Rogers, *Small* **2018**, *1703334*, 1.
- [54] K. Kwon, J. U. Kim, Y. Deng, S. R. Krishnan, J. Choi, H. Jang, K. Lee, C.-J. Su, I. Yoo,

- Y. Wu, L. Lipschultz, J.-H. Kim, T. S. Chung, D. Wu, Y. Park, T. Kim, R. Ghaffari, S. Lee, Y. Huang, J. A. Rogers, *Nat. Electron.* **2021**, *4*, 302.
- [55] J. T. Reeder, J. Choi, Y. Xue, P. Gutruf, J. Hanson, M. Liu, T. Ray, A. J. Bando, R. Avila, W. Xia, S. Krishnan, S. Xu, K. Barnes, M. Pahnke, R. Ghaffari, Y. Huang, J. A. Rogers, *Sci. Adv.* **2019**, *5*, eaau6356.
- [56] C. W. Bae, P. T. Toi, B. Y. Kim, W. Il Lee, H. B. Lee, A. Hanif, E. H. Lee, N. E. Lee, *ACS Appl. Mater. Interfaces* **2019**, *11*, 14567.
- [57] R. M. Torrente-Rodríguez, J. Tu, Y. Yang, J. Min, M. Wang, Y. Song, Y. Yu, C. Xu, C. Ye, W. W. IsHak, W. Gao, *Matter* **2020**, *2*, 921.
- [58] R. Vinoth, T. Nakagawa, J. Mathiyarasu, A. M. V. Mohan, *ACS Sensors* **2021**, *6*, 1174.
- [59] H. Y. Y. Nyein, L. C. Tai, Q. P. Ngo, M. Chao, G. B. Zhang, W. Gao, M. Bariya, J. Bullock, H. Kim, H. M. Fahad, A. Javey, *ACS Sensors* **2018**, *3*, 944.
- [60] G. M. Whitesides, *Nature* **2006**, *442*, 368.
- [61] J. Zhang, S. Yan, D. Yuan, G. Alici, N.-T. Nguyen, M. Ebrahimi Warkiani, W. Li, *Lab Chip* **2016**, *16*, 10.
- [62] K. Sato, W. H. Kang, K. Saga, K. T. Sato, *J. Am. Acad. Dermatol.* **1989**, *20*, 537.
- [63] S. Li, K. Hart, N. Norton, C. A. Ryan, L. Guglani, M. R. Prausnitz, *Bioeng. Transl. Med.* **2021**, *6*, 1.
- [64] D. Vairo, L. Bruzzese, M. Marlinge, L. Fuster, N. Adjriou, N. Kipson, P. Brunet, J. Cautela, Y. Jammes, G. Mottola, S. Burtey, J. Ruf, R. Guieu, E. Fenouillet, *Sci. Rep.* **2017**, *7*, 1.
- [65] H. Hojaiji, Y. Zhao, M. C. Gong, M. Mallajosyula, J. Tan, H. Lin, A. M. Hojaiji, S. Lin, C. Milla, A. M. Madni, S. Emaminejad, *Lab Chip* **2020**, *20*, 4582.
- [66] M. Wang, Y. Yang, J. Min, Y. Song, J. Tu, D. Mukasa, C. Ye, C. Xu, N. Heflin, J. S. McCune, T. K. Hsiai, Z. Li, W. Gao, *Nat. Biomed. Eng.* **2022**, DOI 10.1038/s41551-022-00916-z.

- [67] X. Xuan, C. Pérez-Ràfols, C. Chen, M. Cuartero, G. A. Crespo, *ACS Sensors* **2021**, *6*, 2763.
- [68] M. Roustit, S. Blaise, J. L. Cracowski, *Br. J. Clin. Pharmacol.* **2014**, *77*, 63.
- [69] M. Herrero-Fernandez, T. Montero-Vilchez, P. Diaz-Calvillo, M. Romera-Vilchez, A. Buendía-Eisman, S. Arias-Santiago, *J. Clin. Med.* **2022**, *11*, 298.
- [70] M. Bariya, L. Li, R. Ghattamaneni, C. H. Ahn, H. Y. Y. Nyein, L. C. Tai, A. Javey, *Sci. Adv.* **2020**, *6*, 1.
- [71] H. Fruhstorfer, U. Abel, C.-D. Garthe, A. , *Clin. Anat.* **2000**, *13*, 429.
- [72] Z. Xu, J. Li, H. Zhou, X. Jiang, C. Yang, F. Wang, Y. Pan, N. Li, X. Li, L. Shi, X. Shi, *RSC Adv.* **2016**, *6*, 43626.
- [73] J. Yang, H. C. Cramer, E. C. Bremer, S. Buyukozturk, Y. Yin, C. Franck, *Extrem. Mech. Lett.* **2022**, *51*, 101572.
- [74] L. Wang, T. Xu, X. Zhang, *TrAC - Trends Anal. Chem.* **2021**, *134*, 116130.
- [75] D. J. Beebe, G. A. Mensing, G. M. Walker, *Annu. Rev. Biomed. Eng.* **2002**, *4*, 261.
- [76] A. R. Wheeler, W. R. Thronset, R. J. Whelan, A. M. Leach, R. N. Zare, Y. H. Liao, K. Farrell, I. D. Manger, A. Daridon, *Anal. Chem.* **2003**, *75*, 3581.
- [77] J. R. Sempionatto, A. Martin, L. García-Carmona, A. Barfidokht, J. F. Kurniawan, J. R. Moreto, G. Tang, A. Shin, X. Liu, A. Escarpa, J. Wang, *Electroanalysis* **2019**, *31*, 239.
- [78] A. Hauke, P. Simmers, Y. R. Ojha, B. D. Cameron, R. Ballweg, T. Zhang, N. Twine, M. Brothers, E. Gomez, J. Heikenfeld, *Lab Chip* **2018**, *18*, 3750.
- [79] A. J. Bandodkar, P. Gutruf, J. Choi, K. Lee, Y. Sekine, J. T. Reeder, W. J. Jeang, A. J. Aranyosi, S. P. Lee, J. B. Model, R. Ghaffari, C.-J. Su, J. P. Leshock, T. Ray, A. Verrillo, K. Thomas, V. Krishnamurthi, S. Han, J. Kim, S. Krishnan, T. Hang, J. A. Rogers, *Sci. Adv.* **2019**, *5*, eaav3294.
- [80] A. J. Bandodkar, J. Choi, S. P. Lee, W. J. Jeang, P. Agyare, P. Gutruf, S. Wang, R. A. Sponenburg, J. T. Reeder, S. Schon, T. R. Ray, S. Chen, S. Mehta, S. Ruiz, J. A. Rogers,

- Adv. Mater.* **2019**, *31*, 1902109.
- [81] Z. Yuan, L. Hou, M. Bariya, H. Y. Y. Nyein, L. C. Tai, W. Ji, L. Li, A. Javey, *Lab Chip* **2019**, *19*, 3179.
- [82] H. Y. Y. Nyein, M. Bariya, L. Kivimäki, S. Uusitalo, T. S. Liaw, E. Jansson, C. H. Ahn, J. A. Hangasky, J. Zhao, Y. Lin, T. Happonen, M. Chao, C. Liedert, Y. Zhao, L. Tai, J. Hiltunen, A. Javey, *Sci. Adv.* **2019**, *5*, DOI 10.1126/sciadv.aaw9906.
- [83] A. R. Naik, Y. Zhou, A. A. Dey, D. L. G. Arellano, U. Okoroanyanwu, E. B. Secor, M. C. Hersam, J. Morse, J. P. Rothstein, K. R. Carter, J. J. Watkins, *Lab Chip* **2022**, *22*, 156.
- [84] L. B. Baker, J. B. Model, K. A. Barnes, M. L. Anderson, S. P. Lee, K. A. Lee, S. D. Brown, A. J. Reimel, T. J. Roberts, R. P. Nuccio, J. L. Bonsignore, C. T. Ungaro, J. M. Carter, W. Li, M. S. Seib, J. T. Reeder, A. J. Aranyosi, J. A. Rogers, R. Ghaffari, *Sci. Adv.* **2020**, *6*, 17.
- [85] P. Pirovano, M. Dorrian, A. Shinde, A. Donohoe, A. J. Brady, N. M. Moyna, G. Wallace, D. Diamond, M. McCaul, *Talanta* **2020**, *219*, 121145.
- [86] Q. Cao, B. Liang, X. Mao, J. Wei, T. Tu, L. Fang, X. Ye, *Electroanalysis* **2021**, *33*, 643.
- [87] H. Cho, H. Y. Kim, J. Y. Kang, T. S. Kim, *J. Colloid Interface Sci.* **2007**, *306*, 379.
- [88] H. Zhang, Y. Qiu, S. Yu, C. Ding, J. Hu, H. Qi, Y. Tian, Z. Zhang, A. Liu, H. Wu, *Biomicrofluidics* **2022**, *16*, 044104.
- [89] J. Son, G. Y. Bae, S. Lee, G. Lee, S. W. Kim, D. Kim, S. Chung, K. Cho, *Adv. Mater.* **2021**, *33*, 2102740.
- [90] H. Lin, J. Tan, J. Zhu, S. Lin, Y. Zhao, W. Yu, H. Hojaiji, B. Wang, S. Yang, X. Cheng, Z. Wang, E. Tang, C. Yeung, S. Emaminejad, *Nat. Commun.* **2020**, *11*, 1.
- [91] J. Choi, S. Chen, Y. Deng, Y. Xue, J. T. Reeder, D. Franklin, Y. S. Oh, J. B. Model, A. J. Aranyosi, S. P. Lee, R. Ghaffari, Y. Huang, J. A. Rogers, *Adv. Healthc. Mater.* **2021**, *10*, 2000722.
- [92] X. He, S. Yang, Q. Pei, Y. Song, C. Liu, T. Xu, X. Zhang, *ACS Sensors* **2020**, *5*, 1548.

- [93] J. Xiao, Y. Liu, L. Su, D. Zhao, L. Zhao, X. Zhang, *Anal. Chem.* **2019**, *91*, 14803.
- [94] H. B. Lee, M. Meeseepong, T. Q. Trung, B. Y. Kim, N. E. Lee, *Biosens. Bioelectron.* **2020**, *156*, 112133.
- [95] C. K. Camplisson, K. M. Schilling, W. L. Pedrotti, H. A. Stone, A. W. Martinez, *Lab Chip* **2015**, *15*, 4461.
- [96] J. Songok, M. Toivakka, *ACS Appl. Mater. Interfaces* **2016**, *8*, 30523.
- [97] T. D. Wheeler, A. D. Stroock, *Nature* **2008**, *455*, 208.
- [98] N. S. Lynn, D. S. Dandy, *Lab Chip* **2009**, *9*, 3422.
- [99] X. Chen, Y. Li, D. Han, H. Zhu, C. Xue, H. Chui, T. Cao, K. Qin, *Micromachines* **2019**, *10*, 457.
- [100] S. B. Kim, K. H. Lee, M. S. Raj, B. Lee, J. T. Reeder, J. Koo, A. Hourlier-Fargette, A. J. Bhandodkar, S. M. Won, Y. Sekine, J. Choi, Y. Zhang, J. Yoon, B. H. Kim, Y. Yun, S. Lee, J. Shin, J. Kim, R. Ghaffari, J. A. Rogers, *Small* **2018**, *14*, 1.
- [101] J. A. Rogers, S. Y. Sekine, Y. Sekine, S. B. Kim, Y. Zhang, A. J. Bhandodkar, S. Xu, J. Choi, M. Irie, T. R. Ray, P. Kohli, N. Kozai, T. Sugita, Y. Wu, K. Lee, K.-T. Lee, R. Ghaffari, *Lab Chip* **2018**, *18*, 2178.
- [102] L. B. Baker, M. S. Seib, K. A. Barnes, S. D. Brown, M. A. King, P. J. D. De Chavez, S. Qu, J. Archer, A. S. Wolfe, J. R. Stofan, J. M. Carter, D. E. Wright, J. Wallace, D. S. Yang, S. Liu, J. Anderson, T. Fort, W. Li, J. A. Wright, S. P. Lee, J. B. Model, J. A. Rogers, A. J. Aranyosi, R. Ghaffari, *Adv. Mater. Technol.* **2022**, *2200249*, 2200249.
- [103] A. R. Carr, Y. H. Patel, C. R. Neff, S. Charkhabi, N. E. Kallmyer, H. F. Angus, N. F. Reuel, *npj Digit. Med.* **2020**, *3*, 62.
- [104] H. Yoon, J. Nah, H. Kim, S. Ko, M. Sharifuzzaman, S. C. Barman, X. Xuan, J. Kim, J. Y. Park, *Sensors Actuators, B Chem.* **2020**, *311*, DOI 10.1016/j.snb.2020.127866.
- [105] F. M. Vivaldi, A. Dallinger, A. Bonini, N. Poma, L. Sembranti, D. Biagini, P. Salvo, F. Greco, F. Di Francesco, *ACS Appl. Mater. Interfaces* **2021**, *13*, 30245.

- [106] J. R. Sempionatto, M. Lin, L. Yin, E. De la paz, K. Pei, T. Sonsa-ard, A. N. de Loyola Silva, A. A. Khorshed, F. Zhang, N. Tostado, S. Xu, J. Wang, *Nat. Biomed. Eng.* **2021**, *5*, 737.
- [107] S. Lin, J. Zhu, W. Yu, B. Wang, K. A. Sabet, Y. Zhao, X. Cheng, H. Hojaiji, H. Lin, J. Tan, C. Milla, R. W. Davis, S. Emaminejad, *Proc. Natl. Acad. Sci.* **2022**, *119*, DOI 10.1073/pnas.2201937119.
- [108] J. R. Sempionatto, V. R. V. Montiel, E. Vargas, H. Teymourian, J. Wang, *ACS Sensors* **2021**, *6*, 1745.
- [109] A. K. Yousafzai, M. A. Rasheed, Z. A. Bhutta, *J. Child Psychol. Psychiatry Allied Discip.* **2013**, *54*, 367.
- [110] A. M. V. Mohan, B. Brunetti, A. Bulbarelo, J. Wang, *Analyst* **2015**, *140*, 7522.
- [111] M. Gleeson, D. C. Nieman, B. K. Pedersen, *J. Sports Sci.* **2004**, *22*, 115.
- [112] H. Teymourian, C. Moonla, F. Tehrani, E. Vargas, R. Aghavali, A. Barfidokht, T. Tangkuaram, P. P. Mercier, E. Dassau, J. Wang, *Anal. Chem.* **2020**, *92*, 2291.
- [113] K. S. Eom, Y. J. Lee, H. W. Seo, J. Y. Kang, J. S. Shim, S. H. Lee, *Analyst* **2020**, *145*, 908.
- [114] A. J. Bandothkar, J. Wang, *Electroanalysis* **2016**, *28*, 1188.
- [115] W. Jia, G. Valdés-Ramírez, A. J. Bandothkar, J. R. Windmiller, J. Wang, *Angew. Chemie - Int. Ed.* **2013**, *52*, 7233.
- [116] A. J. Bandothkar, J.-M. You, N.-H. Kim, Y. Gu, R. Kumar, A. M. V. Mohan, J. Kurniawan, S. Imani, T. Nakagawa, B. Parish, M. Parthasarathy, P. P. Mercier, S. Xu, J. Wang, *Energy Environ. Sci.* **2017**, *10*, 1581.
- [117] J. Lv, I. Jeerapan, F. Tehrani, L. Yin, C. A. Silva-Lopez, J. H. Jang, D. Joshua, R. Shah, Y. Liang, L. Xie, F. Soto, C. Chen, E. Karshalev, C. Kong, Z. Yang, J. Wang, *Energy Environ. Sci.* **2018**, *11*, 3431.
- [118] J. Lv, L. Yin, X. Chen, I. Jeerapan, C. A. Silva, Y. Li, M. Le, Z. Lin, L. Wang, A. Trifonov, S. Xu, S. Cosnier, J. Wang, *Adv. Funct. Mater.* **2021**, *31*, 1.

- [119] M. J. Patterson, S. D. R. Galloway, M. A. Nimmo, *Exp. Physiol.* **2000**, 85, 869.
- [120] H. K. Walker, W. D. Hall, J. W. Hurst, *Clinical Methods*, Butterworths, **1990**.
- [121] B. Paul, S. Demuru, C. Lafaye, M. Saubade, D. Briand, *Adv. Mater. Technol.* **2021**, 6, 1.
- [122] M. Parrilla, I. Ortiz-Gómez, R. Cánovas, A. Salinas-Castillo, M. Cuartero, G. A. Crespo, *Anal. Chem.* **2019**, 91, 8644.
- [123] J. Wei, X. Zhang, S. M. Mugo, Q. Zhang, *Anal. Chem.* **2022**, DOI 10.1021/ACS.ANALCHEM.2C02587.
- [124] L. B. Baker, M. A. King, D. M. Keyes, S. D. Brown, M. D. Engel, M. S. Seib, A. J. Aranyosi, R. Ghaffari, *Int. J. Sport Nutr. Exerc. Metab.* **2022**, 32, 342.
- [125] A. S. M. Steijlen, K. M. B. Jansen, J. Bastemeijer, P. J. French, A. Bossche, *Anal. Chem.* **2022**, 17, 36.
- [126] B. Paul Kunnel, S. Demuru, *Lab Chip* **2022**, 22, 1793.
- [127] K. Sato, *Rev. Physiol. Biochem. Pharmacol.* **1977**, 79, 51.
- [128] J. Wang, L. Wang, G. Li, D. Yan, C. Liu, T. Xu, X. Zhang, *ACS Sensors* **2022**, 7, 3102.
- [129] K. Zhang, J. Zhang, F. Wang, D. Kong, *ACS Sensors* **2021**, 6, 2261.
- [130] J. A. Yee, *Ref. Modul. Biomed. Sci.* **2015**, DOI 10.1016/B978-0-12-801238-3.05068-6.
- [131] G. Yosipovitch, J. Reis, E. Tur, H. Blau, D. Harell, G. Morduchowicz, G. Boner, *J. Lab. Clin. Med.* **1994**, 124, 808.
- [132] J. Kim, Y. Wu, H. Luan, D. S. Yang, D. Cho, S. S. Kwak, S. Liu, H. Ryu, R. Ghaffari, J. A. Rogers, J. Kim, Y. Wu, H. Luan, D. S. Yang, D. Cho, S. S. Kwak, S. Liu, H. Ryu, R. Ghaffari, J. A. Rogers, *Adv. Sci.* **2022**, 9, 1.
- [133] D. Czarnowski, J. Górski, J. Józwiuk, A. Boroń-Kaczmarek, *Eur. J. Appl. Physiol. Occup. Physiol.* **1992**, 65, 135.
- [134] T. Guinovart, A. J. Bandodkar, J. R. Windmiller, F. J. Andrade, J. Wang, *Analyst* **2013**, 138, 7031.

- [135] S. T. Keene, D. Fogarty, R. Cooke, C. D. Casadevall, A. Salleo, O. Parlak, *Adv. Healthc. Mater.* **2019**, *8*, 1901321.
- [136] L. H. An'd Jan-Bjirn, *J. Appl. Physiol.* **1972**, *32*.
- [137] H. Shen, H. Lei, M. Gu, S. Miao, Z. Gao, X. Sun, L. Sun, G. Chen, H. Huang, L. Chen, Z. Wen, H. Shen, M. Gu, S. Miao, L. Sun, H. Huang, L. Chen, H. Lei, Z. Gao, X. Sun, Z. Wen, G. Chen, *Adv. Funct. Mater.* **2022**, *32*, 2204525.
- [138] L. Chen, F. Chen, G. Liu, H. Lin, Y. Bao, D. Han, W. Wang, Y. Ma, B. Zhang, L. Niu, *Anal. Chem.* **2022**, DOI 10.1021/ACS.ANALCHEM.2C00684.
- [139] H. Lee, Y. J. Hong, S. Baik, T. Hyeon, D. H. Kim, *Adv. Healthc. Mater.* **2018**, *7*, 1.
- [140] J. Moyer, D. Wilson, I. Finkelshtein, B. Wong, R. Potts, *Diabetes Technol. Ther.* **2012**, *14*, 398.
- [141] H. Mirzajani, T. Abbasiasl, F. Mirlou, E. Istif, M. J. Bathaei, Ç. Dağ, O. Deyneli, D. Yazıcı, L. Beker, *Biosens. Bioelectron.* **2022**, *213*, DOI 10.1016/j.bios.2022.114450.
- [142] P. H. Lin, S. C. Sheu, C. W. Chen, S. C. Huang, B. R. Li, *Talanta* **2022**, *241*, 123187.
- [143] P. Mengarda, F. A. L. Dias, J. V. C. Peixoto, R. Osiecki, M. F. Bergamini, L. H. Marcolino-Junior, *Sensors Actuators B Chem.* **2019**, *296*, 126663.
- [144] K. Van Hoovels, X. Xuan, M. Cuartero, M. Gijssels, M. Swarén, G. A. Crespo, *ACS Sensors* **2021**, *6*, 3496.
- [145] P. Kanokpaka, L. Y. Chang, B. C. Wang, T. H. Huang, M. J. Shih, W. S. Hung, J. Y. Lai, K. C. Ho, M. H. Yeh, *Nano Energy* **2022**, *100*, 107464.
- [146] E. V. Daboss, D. V. Tikhonov, E. V. Shcherbacheva, A. A. Karyakin, *Anal. Chem.* **2022**, *94*, 9201.
- [147] K. Khemtonglang, N. Chaiyaphet, T. Kumsaen, C. Chaiyachati, O. Chuchuen, *Sensors* **2022**, *Vol. 22, Page 6435* **2022**, *22*, 6435.
- [148] M. J. Buono, *Exp. Physiol.* **1999**, *84*, 401.
- [149] C. Huang, M. Chen, L. Huang, I. Mao, *Chin. J. Physiol.* **2002**, *45*, 115.

- [150] X. Yang, J. Yi, T. Wang, Y. Feng, J. Wang, J. Yu, F. Zhang, Z. Jiang, Z. Lv, H. Li, T. Huang, D. Si, X. Wang, R. Cao, X. Chen, *Adv. Mater.* **2022**, 2201768.
- [151] X. Pei, M. Sun, J. Wang, J. Bai, X. Bo, M. Zhou, X. Pei, M. Sun, J. Wang, J. Bai, X. Bo, M. Zhou, *Small* **2022**, 2205061.
- [152] J. Zhao, H. Yin Yin Nyein, L. Hou, Y. Lin, M. Bariya, C. Heera Ahn, W. Ji, Z. Fan, A. Javey, J. Zhao, H. Y. Y Nyein, L. Hou, Y. Lin, M. Bariya, C. H. Ahn, W. Ji, A. Javey, A. Javey Berkeley Sensor, A. Center, Z. Fan, *Adv. Mater.* **2021**, 33, 2006444.
- [153] E. Russell, G. Koren, M. Rieder, S. H. M. Van Uum, *Ther. Drug Monit.* **2014**, 36, 30.
- [154] M. Zea, F. G. Bellagambi, H. Ben Halima, N. Zine, N. Jaffrezic-Renault, R. Villa, G. Gabriel, A. Errachid, *TrAC - Trends Anal. Chem.* **2020**, 132, 116058.
- [155] T. Laochai, J. Yukird, N. Promphet, J. Qin, O. Chailapakul, N. Rodthongkum, *Biosens. Bioelectron.* **2022**, 203, 114039.
- [156] S. Demuru, J. Kim, M. El Chazli, S. Bruce, M. Dupertuis, P. A. Binz, M. Saubade, C. Lafaye, D. Briand, *ACS Sensors* **2022**, 7, DOI 10.1021/ACSSENSORS.2C01250.
- [157] E. M. R. Kovacs, J. H. C. H. Stegen, F. Brouns, *J. Appl. Physiol.* **1998**, 85, 709.
- [158] J. Brunmair, M. Gotsmy, L. Niederstaetter, B. Neuditschko, A. Bileck, A. Slany, M. L. Feuerstein, C. Langbauer, L. Janker, J. Zanghellini, S. M. Meier-Menches, C. Gerner, *Nat. Commun.* **2021**, 12, DOI 10.1038/S41467-021-26245-4.
- [159] G. Cizza, A. H. Marques, F. Eskandari, I. C. Christie, S. Torvik, M. N. Silverman, T. M. Phillips, E. M. Sternberg, *Biol. Psychiatry* **2008**, 64, 907.
- [160] B. J. Sanghavi, W. Varhue, J. L. Chávez, C. F. Chou, N. S. Swami, *Anal. Chem.* **2014**, 86, 4120.
- [161] N. K. M. Churcher, S. Upasham, P. Rice, C. F. Greyling, S. Prasad, *Electroanalysis* **2022**, 34, 375.
- [162] M. Tsunoda, M. Hirayama, T. Tsuda, K. Ohno, *Clin. Chim. Acta* **2015**, 442, 52.
- [163] A. A. Othman, M. Rosebraugh, K. Chatamra, C. Locke, S. Dutta, *J. Parkinsons. Dis.*

2017, *7*, 275.

- [164] L. C. Tai, T. S. Liaw, Y. Lin, H. Y. Y. Nyein, M. Bariya, W. Ji, M. Hettick, C. Zhao, J. Zhao, L. Hou, Z. Yuan, Z. Fan, A. Javey, *Nano Lett.* **2019**, *19*, 6346.
- [165] J. Xiao, C. Fan, T. Xu, L. Su, X. Zhang, *Sensors Actuators B Chem.* **2022**, *359*, 131586.
- [166] S. Karvinen, T. Sievänen, J. E. Karppinen, P. Hautasaari, G. Bart, A. Samoylenko, S. J. Vainio, J. P. Ahtiainen, E. K. Laakkonen, U. M. Kujala, *Front. Physiol.* **2020**, *11*, 676.
- [167] M. L. Goodwin, J. E. Harris, A. Hernández, L. B. Gladden, *J. Diabetes Sci. Technol.* **2007**, *1*, 558.
- [168] A. Tripathi, K. D. Harris, A. L. Elias, *ACS Omega* **2020**, *5*, 9123.
- [169] A. Tripathi, K. D. Harris, A. L. Elias, *PLoS One* **2021**, *16*, e0257777.

Author Biography



Tamoghna Saha is currently a postdoctoral scholar in the Department of Nanoengineering at the University of California, San Diego (UCSD) working with Prof. Joseph Wang since Feb. 2022. He received his PhD in Chemical and Biomolecular Engineering from North Carolina State University in Jan. 2022 under the supervision of Prof. Orlin D. Velev and Prof. Michael D. Dickey. His PhD research focused on developing wearable sweat based epidermal patches for lactate sensing that functioned on novel fluid withdrawing techniques.



Rafael Del Caño received his PhD in Chemistry from University of Córdoba in 2019, under the mentorship of Teresa Pineda. Afterwards, he made a postdoctoral stage in Encarnación Lorenzo's group at the Autonomous University of Madrid. He is currently postdoctoral researcher at Dr. Joseph Wang's group at the University of California, San Diego after received a postdoctoral fellowship from the University of Córdoba. His current research direction is the design of new electrochemical and wearable biosensors, and the improvement of the analytical and physicochemical properties of the developed devices.



Ernesto De la Paz obtained his B.S in Nanoengineering from Tijuana Institute of Technology (ITT), Mexico in 2016. Later, he obtained his M.S degree in Nanoengineering from the University of California, San Diego (UCSD) in 2019. He is currently pursuing his PhD in Nanoengineering under the supervision of Prof. Joseph Wang. His research focuses on the development of non-invasive wearable electrochemical biosensors that monitor biomarkers of interest from the human body.



Samar S. Sandhu obtained his B.Tech in Engineering Physics from Delhi Technological University (DTU), India in 2018. He then obtained his MS in Nanoengineering from the University of California San Diego (UCSD), where he is currently pursuing his PhD in Nanoengineering under the mentorship of Prof. Joseph Wang. His research focuses on portable and wearable electrochemical sensors for multiphasic field detection of chemical warfare agents, and wearable bioenergy microgrid systems for epidermal sweat sensing.



Joseph Wang is a Distinguished Professor, SAIC Endowed Chair and former Chair of the Department of Nanoengineering at UCSD. He held the Regents Professorship at NMSU and served as the Director of the Center for Bioelectronics at Arizona State University as well as the Editor-in-Chief of *Electroanalysis* (Wiley). He has received several national ACS, ECS & SEAC awards, 10 honorary professorships, and is a fellow of the ECS, RSC & AIMBE. His scientific interests focus on nanomachines, bioelectronics, biosensors, wearable devices, and bionanotechnology.